
FAIRNESS-AWARE DOMAIN GENERALIZATION UNDER COVARIATE AND DEPENDENCE SHIFTS

Chen Zhao
Baylor University
Waco, Texas
chen_zhao@baylor.edu

Kai Jiang
The University of Texas at Dallas
Richardson, Texas
kai.jiang@utdallas.edu

Xintao Wu
University of Arkansas
Fayetteville, Arkansas
xintaowu@uark.edu

Haoliang Wang
The University of Texas at Dallas
Richardson, Texas
haoliang.wang@utdallas.edu

Latifur Khan
The University of Texas at Dallas
Richardson, Texas
lkhan@utdallas.edu

Christan Grant
University of Florida
Gainesville, Florida
christan@ufl.edu

Feng Chen
The University of Texas at Dallas
Richardson, Texas
feng.chen@utdallas.edu

ABSTRACT

Achieving the generalization of an invariant classifier from source domains to shifted target domains while simultaneously considering model fairness is a substantial and complex challenge in machine learning. Existing domain generalization research typically attributes domain shifts to concept shift, which relates to alterations in class labels, and covariate shift, which pertains to variations in data styles. In this paper, by introducing another form of distribution shift, known as dependence shift, which involves variations in fair dependence patterns across domains, we propose a novel domain generalization approach that addresses domain shifts by considering both covariate and dependence shifts. We assert the existence of an underlying transformation model can transform data from one domain to another. By generating data in synthetic domains through the model, a fairness-aware invariant classifier is learned that enforces both model accuracy and fairness in unseen domains. Extensive empirical studies on four benchmark datasets demonstrate that our approach surpasses state-of-the-art methods.

1 Introduction

While modern fairness-aware machine learning techniques have demonstrated significant success in various applications [1, 2, 3], their primary objective is to facilitate equitable decision-making, ensuring fairness across all demographic groups, regardless of sensitive attributes, such as race and gender. Nevertheless, state-of-the-art methods can encounter severe shortcomings during the inference phase, mainly due to poor generalization when the spurious correlation deviates from the patterns seen in the training data. This correlation can manifest either between model outcomes and sensitive attributes [4, 5] or between model outcomes and non-semantic data features [6]. This issue originates from the existence of out-of-distribution (OOD) data, resulting in catastrophic failures.

Over the past decade, the machine learning community has made significant strides in studying the OOD generalization (or domain generalization, DG) problem and attributing the cause of the poor generalization to the distribution shifts from source domains to target domains. There are two dominant shift types [7]: concept shift and covariate shift. Concept shift refers to OOD samples drawn from a distribution with semantic change *e.g.*, *dog v.s. cat*, and covariate shift characterizes the extent to which the distributions of data features differ across domains *e.g.*, *photo v.s. cartoon*.

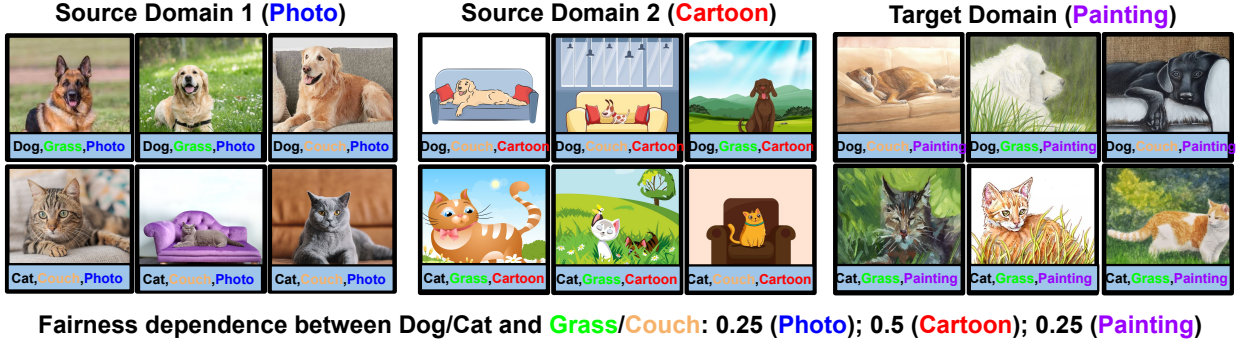


Figure 1: Illustration of fairness-aware domain generalization problems. Different data domains correspond to different image styles (“Photo”, “Cartoon”, and “Painting”). Each domain is associated with various fair dependencies between class labels (“Dog” and “Cat”) and sensitive attributes (“Grass” and “Couch”), estimated using the demographic parity in Appendix C.3. In the Photo domain, (mostly) dogs in the grass and cats in couches. In the Painting domain, (mostly) dogs in couches and cats in the grass.

While a variety of DG approaches have been explored, these methods often exhibit two specific limitations: (1) they predominantly address a single type of distribution shift (either concept or covariate shift) and disregard the significance of integrating fairness considerations into the learning process [8, 9, 10, 11, 12, 13], or (2) existing methods assume that the mentioned distribution shifts remain static, and there exist distinct fairness dependence between model outcomes and sensitive attributes in the source and target domains [4, 5]. Recently, *Pham et al.*, [6] address the DG problem with a focus on model fairness and accuracy in the presence of covariate shift. However, this work assumes that the fair dependence patterns across domains remain constant. Hence, there is a need for research that delves into the fairness-aware DG problem in the context of covariate shift and accounts for the varying fairness dependence between source and target domains. Details and more related works are summarized in Appendix A.

In this paper, in addition to concept shift and covariate shift, inspired by [4], we first introduce a novel type of shift known as “dependence shift” for DG problems. The dependence shift is characterized by a disparity in the dependence between sensitive attributes and sample classes within source domains as compared to target domains. As illustrated in Fig. 1, in the source domain 1, images labeled with “Dog” exhibit a strong correlation with the sensitive attribute “Grass”, whereas “Cat” images are correlated with “Couch”. However, in the target domain, this correlation between image labels and sensitive attributes is reversed and shifted from source domains. Furthermore, we define the fairness-aware DG problem within a broader context, where we account for two types of shifts, covariate shift and dependence shift, that occur when transferring from observed source domains to an unknown and inaccessible target domain. As shown in Fig. 1, various image styles (“Photo”, “Cartoon” and “Painting”) specify different data domains, and “Grass” and “Couch” correspond to sensitive attributes. The goal of the problem is to find a classifier that remains invariant in classifying between “Dog” and “Cat” across the observed source domains and subsequently enhance its generalization performance when faced with a target domain that is unseen during training characterized by different stylistic variations and fairness dependencies. To tackle the problem, we introduce a new framework, which we called *Fair Disentangled Domain Generalization* (FDDG). The key idea in our framework revolves around understanding transformations that account for both covariate and dependence shifts, enabling the mapping of data between domains, and then subsequently enforcing invariance by generating synthetic domains through these transformations. We leverage this framework to systematically define the fairness-aware DG problem as a semi-infinite constrained optimization problem. We then apply this re-formulation to demonstrate that a tight approximation of the problem can be achieved by solving the empirical, parameterized dual for this problem. Moreover, we develop a novel interpretable bound focusing on fairness within a target domain, considering the DG arising from both covariate and dependence shifts. Finally, extensive experimental results on the proposed new algorithm show that our algorithm significantly outperforms state-of-the-art baselines on several benchmarks.

Contributions. Our main contributions are summarized

- To our knowledge, we are the first to introduce a fairness-aware DG problem within a framework that accommodates inter-domain variations arising from two distinct types of distribution shifts, covariate shift and dependence shift.
- We reformulate the problem to a novel constrained learning problem. We further establish duality gap bounds for the empirically parameterized dual of this problem and develop a novel upper bound that specifically

addresses fairness within a target domain while accounting for the domain generalization stemming from both covariate and dependence shifts.

- We present a novel algorithm designed to address the fairness-aware DG problem. This algorithm enforces invariance across unseen target domains by utilizing generative models derived from the observed source domains.
- Comprehensive experiments are conducted to verify the effectiveness of FDDG. We empirically show that our algorithm significantly outperforms state-of-the-art baselines on four benchmarks.

2 Preliminaries

Notations. Let $\mathcal{X} \subseteq \mathbb{R}^d$ denote a feature space, $\mathcal{Z} = \{-1, 1\}$ is a sensitive label space, and $\mathcal{Y} = \{0, 1\}$ is a label space for classification. Let $\mathcal{C} \subseteq \mathbb{R}^c$, $\mathcal{A} \subseteq \mathbb{R}^a$, and $\mathcal{S} \subseteq \mathbb{R}^s$ be the latent content, sensitive and style spaces, respectively, induced from \mathcal{X} and \mathcal{A} by an underlying transformation model $T : \mathcal{X} \times \mathcal{Z} \times \mathcal{E} \rightarrow \mathcal{X} \times \mathcal{Z}$. We use X, Z, Y, C, A, S to denote random variables that take values in $\mathcal{X}, \mathcal{Z}, \mathcal{Y}, \mathcal{C}, \mathcal{A}, \mathcal{S}$ and $\mathbf{x}, z, y, \mathbf{c}, \mathbf{a}, \mathbf{s}$ the realizations. A domain $e \in \mathcal{E}$ is specified by distribution $\mathbb{P}(X^e, Z^e, Y^e) : \mathcal{X} \times \mathcal{Z} \times \mathcal{Y} \rightarrow [0, 1]$. A classifier f in a class space \mathcal{F} denotes $f \in \mathcal{F} : \mathcal{X} \rightarrow \mathcal{Y}$.

Fairness Notions. When learning a fair classifier $f \in \mathcal{F}$ that focuses on statistical parity across different sensitive subgroups, the fairness criteria require the independence between the sensitive random variables Z and the predicted model outcome $f(X)$ [14]. Addressing the issue of preventing group unfairness can be framed as the formulation of a constraint. This constraint mitigates bias by ensuring that $f(X)$ aligns with the ground truth Y , fostering equitable outcomes.

Definition 1 (Group Fairness Notion [3, 15]). *Given a dataset $\mathcal{D} = \{(\mathbf{x}_i, z_i, y_i)\}_{i=1}^{|\mathcal{D}|}$ sampled i.i.d. from $\mathbb{P}(X, Z, Y)$, a classifier $f \in \mathcal{F} : \mathcal{X} \rightarrow \mathcal{Y}$ is fair when the prediction $\hat{Y} = f(X)$ is independent of sensitive random variable Z . To get rid of the indicator function and relax the exact values, a linear approximated form of the difference between sensitive subgroups is defined as*

$$\rho(\hat{Y}, Z) = |\mathbb{E}_{\mathbb{P}(X, Z)} g(\hat{Y}, Z)| \quad \text{where} \quad g(\hat{Y}, Z) = \frac{1}{p_1(1-p_1)} \left(\frac{Z+1}{2} - p_1 \right) \hat{Y} \quad (1)$$

p_1 and $1-p_1$ are the proportion of samples in the subgroup $Z = 1$ and $Z = -1$, respectively.

Specifically, when $p_1 = \mathbb{P}(Z = 1)$ and $p_1 = \mathbb{P}(Z = 1, Y = 1)$, the fairness notion $\rho(\hat{Y}, Z)$ is defined as the difference of demographic parity (DP) and the difference of equalized odds (EO), respectively [15]. In the paper, we will present the results under DP, while the framework can be generalized to multi-class, multi-sensitive attributes and other fairness notions. Strictly speaking, a classifier f is fair over subgroups if it satisfies $\rho(\hat{Y}, Z) = 0$.

Problem Setting. We consider a set of data domains \mathcal{E} , where each domain $e \in \mathcal{E}$ corresponds to a distinct data subset $\mathcal{D}^e = \{(\mathbf{x}_i^e, z_i^e, y_i^e)\}_{i=1}^{|\mathcal{D}^e|}$ sampled i.i.d. from $\mathbb{P}(X^e, Z^e, Y^e)$. Given a dataset $\mathcal{D} = \{\mathcal{D}^e\}_{e \in \mathcal{E}}$, it is partitioned into multiple source domains $\mathcal{E}_s \subset \mathcal{E}$ and unknown target domains which are inaccessible during training. Therefore, given samples from finite source domains \mathcal{E}_s , the goal of fairness-aware domain generalization problems is to learn a classifier $f \in \mathcal{F}$ that is generalizable across all possible domains.

Problem 1 (Fairness-aware Domain Generalization). *Let $\mathcal{E}_s \subset \mathcal{E}$ be a finite subset of source domains and assume that, for each $e \in \mathcal{E}_s$, we have access to its corresponding dataset $\mathcal{D}^e = \{(\mathbf{x}_i^e, z_i^e, y_i^e)\}_{i=1}^{|\mathcal{D}^e|}$ sampled i.i.d. from $\mathbb{P}(X^e, Z^e, Y^e)$. Given a classifier set \mathcal{F} and a loss function $\ell : \mathcal{Y} \times \mathcal{Y} \rightarrow \mathbb{R}$, the goal is to learn a fair classifier $f \in \mathcal{F}$ for any $\mathcal{D}^e \in \mathcal{D}_s = \{\mathcal{D}^e\}_{e \in \mathcal{E}_s}$ that minimizes the worst-case risk over all domains in \mathcal{E} satisfying a group fairness constraint:*

$$\min_{f \in \mathcal{F}} \max_{e \in \mathcal{E}} \mathbb{E}_{\mathbb{P}(X^e, Z^e, Y^e)} \ell(f(X^e), Y^e), \quad \text{subject to } \rho(f(X^e), Z^e) = 0. \quad (2)$$

The goal of Prob. 1 is to seek a fair classifier f that generalizes from the given finite set of source domains \mathcal{E}_s to give a good generalization performance on \mathcal{E} . Since we do not assume data from $\mathcal{E} \setminus \mathcal{E}_s$ is accessible, it makes this problem challenging to solve.

Another challenge is how closely the data distributions in unknown target domains match those in the observed source domains. In [7], there are two forms of distribution shifts: concept shift, where the instance conditional distribution $\mathbb{P}(Y^e | X^e, Z^e)$ varies across different domains, and covariate shift, where the marginal distributions over instance $\mathbb{P}(X^e)$ are various. Yet, neither of these shifts captures the degree to which the distribution shifts with regard to model fairness. Therefore, we introduce a novel variation, dependence shift, where the dependence $\rho(Y^e, Z^e)$ between sensitive attributes and sample classes differs across domains.

Definition 2 (Covariate Shift [12] and Dependence Shift). *In Prob. 1, covariate shift occurs when environmental variation is attributed to disparities in the marginal distributions across instances $\{\mathbb{P}(X^e)\}_{e \in \mathcal{E}}$. On the other hand, Prob. 1 exhibits a dependence shift when environmental variation arises from alterations in the sensitive dependence $\rho(Y^e, Z^e)$.*

3 Fairness-aware Disentangled Domain Generalization

DG tasks can generally be characterized by one form of the three distribution shifts. In this paper, we restrict the scope of our framework to focus on Prob. 1 in which inter-domain variation is due to covariate shift and dependence shift simultaneously through an underlying transformation model T .

Assumption 1 (Transformation Model). *We assume that, $\forall e_i, e_j \in \mathcal{E}, e_i \neq e_j$, there exists a measurable function $T : \mathcal{X} \times \mathcal{Z} \times \mathcal{E} \rightarrow \mathcal{X} \times \mathcal{Z}$, referred as transformation model, that transforms instances from domain e_i to e_j , denoted $(X^{e_j}, Z^{e_j}) = T(X^{e_i}, Z^{e_i}, e_j)$.*

Under Assump. 1, a data subset $\mathcal{D}^{e_j} \in \mathcal{D}$ of domain e_j can be regarded as generated from another data subset \mathcal{D}^{e_i} through the transformation model T by altering (X^{e_i}, Z^{e_i}) to (X^{e_j}, Z^{e_j}) . Building upon the insights from existing DG literature [13, 16, 17], we define T with a specific emphasis on disentangling the variation in data features across domains into latent spaces with three factors. For specific information about the design of T and the learning algorithm, please refer to Sec. 4.

Assumption 2 (Multiple Latent Factors). *Given dataset $\mathcal{D}^e = \{(\mathbf{x}_i^e, z_i^e, y_i^e)\}_{i=1}^{|\mathcal{D}^e|}$ sampled i.i.d. from $\mathbb{P}(X^e, Z^e, Y^e)$ in domain $e \in \mathcal{E}$, we assume that each instance \mathbf{x}_i^e is generated from*

- a latent content factor $\mathbf{c} \in \mathcal{C}$, where $\mathcal{C} = \{\mathbf{c}_{y=0}, \mathbf{c}_{y=1}\}$ refers to a content space;
- a latent sensitive factor $\mathbf{a} \in \mathcal{A}$, where $\mathcal{A} = \{\mathbf{a}_{z=1}, \mathbf{a}_{z=-1}\}$ refers to a sensitive space;
- a latent style factor \mathbf{s}^e , where \mathbf{s}^e is specific to the individual domain e .

We assume that the content and sensitive factors in \mathcal{C} and \mathcal{A} do not change across domains. Each domain e over $\mathbb{P}(X^e, Z^e, Y^e)$ is represented by a style factor \mathbf{s}^e and the dependence score $\rho^e = \rho(Y^e, Z^e)$, denoted $e := (\mathbf{s}^e, \rho^e)$, where \mathbf{s}^e and ρ^e are unique to the domain e .

Note that Assump. 2 is similarly related to the one made in [13, 12, 18, 19]. In our paper, with a focus on group fairness, we expand upon the assumptions of existing works by introducing three latent factors. Because we assume the instance conditional distribution $\mathbb{P}(Y|X, Z)$ remains consistent across domains (i.e., there is no concept shift taking place), under Assumps. 1 and 2, if two instances $(\mathbf{x}^{e_i}, z^{e_i}, y)$ and $(\mathbf{x}^{e_j}, z^{e_j}, y)$ where $e_i, e_j \in \mathcal{E}, i \neq j$ share the same class label, then the latter instance can be reconstructed from the former using T . Specifically, T constructs \mathbf{x}^{e_j} using the content factor of \mathbf{x}^{e_i} , the sensitive factor of \mathbf{x}^{e_j} , and the style factor of \mathbf{x}^{e_j} . Additionally, T constructs z^{e_j} by employing the sensitive factor of \mathbf{x}^{e_j} . For fairness-aware invariant learning, we make the following assumption.

Assumption 3 (Fairness-aware Domain Shift). *We assume that inter-domain variation is characterized by the covariate shift and dependence shift in $\mathbb{P}(X^e)$ and $\rho(Y^e, Z^e), \forall e \in \mathcal{E}$. As a consequence, we assume that $\mathbb{P}(Y^e|X^e, Z^e)$ is stable across domains. Given a domain transformation function T , for any $\mathbf{x} \in \mathcal{X}, z \in \mathcal{Z}$, and $y \in \mathcal{Y}$, it holds that*

$$\mathbb{P}(Y^{e_i} = y | X^{e_i} = \mathbf{x}^{e_i}, Z^{e_i} = z^{e_i}) = \mathbb{P}(Y^{e_j} = y | (X^{e_j}, Z^{e_j}) = T(\mathbf{x}^{e_i}, z^{e_i}, e_j)), \forall e_i, e_j \in \mathcal{E}, i \neq j$$

In Assump. 3, the domain shift captured by T would characterize the mapping from the underlying distributions $\mathbb{P}(X^{e_i})$ and $\rho(Y^{e_i}, Z^{e_i})$ over \mathcal{D}^{e_i} to the distribution $\mathbb{P}(X^{e_j})$ and $\rho(Y^{e_j}, Z^{e_j})$ of samples from a different data domain \mathcal{D}^{e_j} , respectively. With this in mind and under Assump. 3, we introduce a new definition of fairness-aware invariance with respect to the variation captured by T and satisfying the group fair constraint introduced in Defn. 1.

Definition 3 (Fairness-aware T -Invariance). *Given a transformation model T , a fairness-aware classifier $f \in \mathcal{F}$ is domain invariant if it holds*

$$f(\mathbf{x}^{e_i}) = f(\mathbf{x}^{e_j}), \quad \text{and} \quad \rho(f(X^{e_i}), Z^{e_i}) = \rho(f(X^{e_j}), Z^{e_j}) = 0 \quad (3)$$

almost surely when $(\mathbf{x}^{e_j}, z^{e_j}) = T(\mathbf{x}^{e_i}, z^{e_i}, e_j)$, $\mathbf{x}^{e_i} \sim \mathbb{P}(X^{e_i})$, $\mathbf{x}^{e_j} \sim \mathbb{P}(X^{e_j})$, and $e_i, e_j \in \mathcal{E}$.

Defn. 3 is crafted to enforce invariance on the predictions generated by f directly. We expect a prediction to yield the same prediction for any realization of data under T while being aware of group fairness.

Problem 2 (Fairness-aware Disentanglement for Domain Generalization). *Under Defn. 3 and Assump. 3, if we restrict \mathcal{F} of Prob. 1 to the set of invariant fairness-aware classifiers, the Prob. 1 is equivalent to the following problem*

$$P^* \triangleq \min_{f \in \mathcal{F}} R(f) \triangleq \mathbb{E}_{\mathbb{P}(X^{e_i}, Z^{e_i}, Y^{e_i})} \ell(f(X^{e_i}), Y^{e_i}) \quad (4)$$

$$\text{subject to } f(\mathbf{x}^{e_i}) = f(\mathbf{x}^{e_j}), \quad \rho(f(X^{e_i}), Z^{e_i}) = \rho(f(X^{e_j}), Z^{e_j}) = 0$$

where $\mathbf{x}^{e_i} \sim \mathbb{P}(X^{e_i})$, $\mathbf{z}^{e_i} \sim \mathbb{P}(Z^{e_i})$, $(\mathbf{x}^{e_j}, \mathbf{z}^{e_j}) = T(\mathbf{x}^{e_i}, \mathbf{z}^{e_i}, e_j)$, $\forall e_i, e_j \in \mathcal{E}$, $i \neq j$.

Similar to [12], Prob. 2 is not a composite optimization problem. Moreover, acquiring domain labels is often expensive or even unattainable, primarily due to privacy concerns. Consequently, under the assumptions of disentanglement-based invariance and domain shift, Problem 1 can be approximated to Problem 2 by removing the max operator. Furthermore, Prob. 2 offers a new and theoretically-principled perspective on Prob. 1, when data varies from domain to domain with respect to an underlying transformation model T . To optimize Prob. 2 is challenging because

- The strict equality constraints in Prob. 2 are difficult to enforce in practice;
- Enforcing constraints on deep networks is known to be a challenging problem due to non-convexity. Simply transforming them to regularization cannot guarantee satisfaction for constrained problems;
- As we have incomplete access to all domains \mathcal{E} or $\mathbb{P}(X, Z, Y)$, it limits the ability to enforce fairness-aware T -invariance and further makes it hard to estimate $R(f)$.

Due to such challenges, we develop a tractable method for approximately solving Prob. 2 with optimality guarantees. To address the first challenge, we relax constraints in Prob. 2

$$P^*(\gamma_1, \gamma_2) \triangleq \min_{f \in \mathcal{F}} R(f) \quad \text{subject to} \quad \delta^{e_i, e_j}(f) \leq \gamma_1, \epsilon^{e_i}(f) \leq \frac{\gamma_2}{2} \text{ and } \epsilon^{e_j}(f) \leq \frac{\gamma_2}{2} \quad (5)$$

where

$$\delta^{e_i, e_j}(f) \triangleq \mathbb{E}_{\mathbb{P}(X, Z)} d[f(X^{e_i}), f(X^{e_j} = T(X^{e_i}, Z^{e_i}, e_j))], \quad (6)$$

$$\epsilon^{e_i}(f) \triangleq \rho(f(X^{e_i}), Z^{e_i}), \quad \epsilon^{e_j}(f) \triangleq \rho(f(X^{e_j}), Z^{e_j}) \quad (7)$$

and $\forall e_i, e_j \in \mathcal{E}$, $i \neq j$. Here, $\gamma_1, \gamma_2 > 0$ are constants controlling the extent of relaxation and $d[\cdot]$ is a distance metric, e.g., KL-divergence. When $\gamma_1 = \gamma_2 = 0$, Eqs. (4) and (5) are equivalent.

Theorem 1 (Fairness Upper Bound of the Unseen Target Domain). *In accordance with Defn. 1 and Eq. (7), for any domain $e \in \mathcal{E}$, the fairness dependence under instance distribution $\mathbb{P}(X^e, Z^e, Y^e)$ with respect to the classifier $f \in \mathcal{F}$ is defined as:*

$$\epsilon^e(f) = |\mathbb{E}_{\mathbb{P}(X^e, Z^e)} g(f(X^e), Z^e)|$$

With observed source domains \mathcal{E}_s , the dependence at any unseen target domain $e_t \in \mathcal{E} \setminus \mathcal{E}_s$ is upper bounded. $D[\cdot]$ is the Jensen-Shannon distance [20] metric.

$$\begin{aligned} \epsilon^{e_t}(f) &\leq \frac{1}{|\mathcal{E}_s|} \sum_{e_i \in \mathcal{E}_s} \epsilon^{e_i}(f) + \sqrt{2} \min_{e_i \in \mathcal{E}_s} D[\mathbb{P}(X^{e_t}, Z^{e_t}, Y^{e_t}), \mathbb{P}(X^{e_i}, Z^{e_i}, Y^{e_i})] \\ &\quad + \sqrt{2} \max_{e_i, e_j \in \mathcal{E}_s} D[\mathbb{P}(X^{e_i}, Z^{e_i}, Y^{e_i}), \mathbb{P}(X^{e_j}, Z^{e_j}, Y^{e_j})] \end{aligned}$$

where $D[\mathbb{P}_1, \mathbb{P}_2] = \sqrt{\frac{1}{2} KL(\mathbb{P}_1 \| \frac{\mathbb{P}_1 + \mathbb{P}_2}{2}) + \frac{1}{2} KL(\mathbb{P}_2 \| \frac{\mathbb{P}_1 + \mathbb{P}_2}{2})}$ is JS divergence defined based on KL divergence.

Since it is unrealistic to have access to the full distribution and we only have access to source domains, given data sampled from \mathcal{E}_s , we consider the empirical dual problem

$$\begin{aligned} D_{\xi, N, \mathcal{E}_s}^*(\gamma_1, \gamma_2) &\triangleq \max_{\lambda_1(e_i, e_j), \lambda_2(e_i, e_j)} \min_{\theta \in \Theta} \hat{R}(\theta) \\ &\quad + \frac{1}{|\mathcal{E}_s|} \sum_{e_i, e_j \in \mathcal{E}_s} \left[\lambda_1(e_i, e_j) (\hat{\delta}^{e_i, e_j}(\theta) - \gamma_1) + \lambda_2(e_i, e_j) (\hat{\epsilon}^{e_i}(\theta) + \hat{\epsilon}^{e_j}(\theta) - \gamma_2) \right] \end{aligned} \quad (8)$$

where $\xi = \mathbb{E}_{\mathbb{P}(X)} \|f(\mathbf{x}) - \hat{f}(\mathbf{x}, \theta)\|_\infty > 0$ is a constant bounding the difference between f and its parameterized counterpart $\hat{f}: \mathcal{X} \times \Theta \rightarrow \mathbb{R}$ defined in the Definition 5.1 of [12]. $\lambda_1(e_i, e_j), \lambda_2(e_i, e_j) > 0$ are dual variables. $\hat{R}(\theta)$, $\hat{\delta}^{e_i, e_j}(\theta)$, $\hat{\epsilon}^{e_i}(\theta)$ and $\hat{\epsilon}^{e_j}(\theta)$ are the empirical counterparts of $R(\hat{f}(\cdot, \theta))$, $\delta^{e_i, e_j}(\hat{f}(\cdot, \theta))$, $\epsilon^{e_i}(\hat{f}(\cdot, \theta))$ and $\epsilon^{e_j}(\hat{f}(\cdot, \theta))$, respectively. With such approximation on the dual problem in Eq. (8), the duality gap between P^* and $D_{\xi, N, \mathcal{E}_s}^*(\gamma_1, \gamma_2)$ can be explicitly bounded.

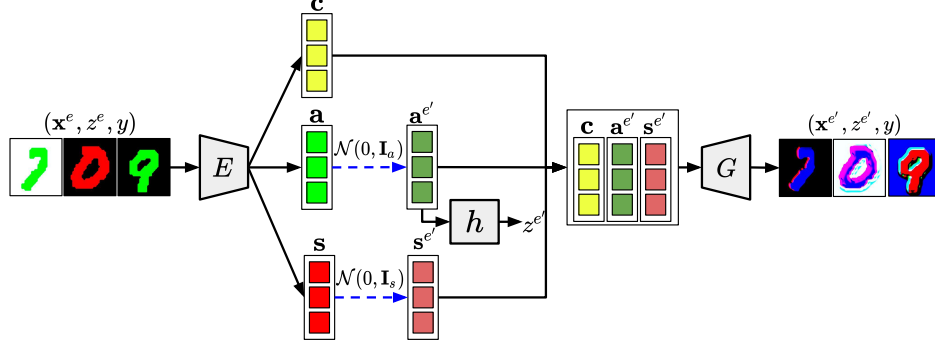


Figure 2: An overview of data generation in synthetic domains via an underlying transformation model T . Data are augmented through T based on invariant content factors and randomly sampled sensitive and style factors that encode synthetic domains. We demonstrate the concept using the CCMNIST introduced in Sec. 5, where the domains are associated with various digit colors and the sensitive labels are determined by the background colors of each image.

Theorem 2 (Fairness-aware Data-dependent Duality Gap). *Given $\xi > 0$, assuming $\{\hat{f}(\cdot, \theta) : \theta \in \Theta\} \subseteq \mathcal{F}$ has finite VC-dimension, with M datapoints sampled from $\mathbb{P}(X, Z, Y)$ we have*

$$|P^* - D_{\xi, N, \mathcal{E}_s}^*(\gamma)| \leq L\|\gamma\|_1 + \xi k(1 + \|\lambda_p^*\|_1) + O(\sqrt{\log(M)/M})$$

where $\gamma = [\gamma_1, \gamma_2]^T$; L is the Lipschitz constant of $P^*(\gamma_1, \gamma_2)$; k is a small universal constant defined in Proposition 3 of Appendix E; and λ_p^* is the optimal dual variable for a perturbed version of Eq. (5).

The duality gap that arises when solving the empirical problem presented in Eq. (8) is minimal when the fairness-aware T -invariance in Defn. 3 margin γ is narrow, and the parametric space closely approximates \mathcal{F} . Proofs of Theorems 1 and 2 are provided in Appendix E.

4 An Effective Algorithm

Fairness-aware DG via T . Motivated by the theoretical insights in Sec. 3, we propose a simple but effective algorithm, namely FDDG. This algorithm consists of two stages. In the first stage, we train the transformation model T using data from the source domains. In the second stage, we harness the power of T to address the unconstrained dual optimization problem outlined in Eq. (8) through a series of primal-dual iterations.

Regarding the architecture of T , we expand upon the networks used in [18] by incorporating an additional output of the encoder $E : \mathcal{X} \times \mathcal{Z} \rightarrow \mathcal{C} \times \mathcal{A} \times \mathcal{S}$ for sensitive factors $\mathbf{a} \in \mathcal{A}$ and including a sensitive classifier $h : \mathcal{A} \rightarrow \mathcal{Z}$. A generator (decoder) $G : \mathcal{C} \times \mathcal{A} \times \mathcal{S} \rightarrow \mathcal{X} \times \mathcal{Z}$ is used to reconstruct instances from encoded latent factors. Following [18, 12], the transformation model T is trained using data in the observed source domains by applying reconstruction of them. Detailed training process of T is provided in Appendix C.

Given the finite number of observed source domains, to enhance the generalization performance for unseen target domains, the invariant classifier \hat{f} is trained by expanding the dataset with synthetic domains. These synthetic domains are created by introducing random instance styles and random fair dependencies within the domain. As described in Fig. 2, the sensitive factor \mathbf{a}^e and the style factor \mathbf{s}^e are randomly sampled from their prior distributions $\mathcal{N}(0, \mathbf{I}_a)$ and $\mathcal{N}(0, \mathbf{I}_s)$, respectively. Along with the unchanged content factor \mathbf{c} , they are further passed through G to generate a new instance within a novel domain. Under Assump. 3 and Defn. 3, according to Eqs. (6) and (7), data augmented in synthetic domains are required to maintain invariance in terms of accuracy and fairness with the data in the corresponding original domains.

Walking Through Algorithm 1. Our proposed implementation is shown in Algorithm 1 to solve the empirical dual Eq. (8). In lines 15-20, we describe the DATAUG procedure that takes an example (\mathbf{x}, z, y) as INPUT and returns an augmented example (\mathbf{x}', z', y) from a new synthetic domain as OUTPUT. The augmented example has the same content factor as the input example but has different sensitive and style factors sampled from their associated prior distributions that encode a new synthetic domain. Lines 1-14 show the main training loop for FDDG. In line 6, for each example in the minibatch \mathcal{B} , we apply the procedure DATAUG to generate an augmented example from a new synthetic domain described above. In line 7, we consider KL-divergence as the distance metric for $d[\cdot]$. All the augmented examples are stored in the set \mathcal{B}' . The Lagrangian dual loss function is defined based on \mathcal{B} and \mathcal{B}' in line 10. The primal parameters θ and the dual parameters λ_1 and λ_2 are updated in lines 11-12.

Algorithm 1 Fair Disentangled Domain Generalization.

Require: Pretained encoder E , decoder G and sensitive classifier h within T .

Initialize: primal and dual learning rate η_p, η_d , empirical constant γ_1, γ_2 .

```
1: repeat
2:   for minibatch  $\mathcal{B} = \{(\mathbf{x}_i, z_i, y_i)\}_{i=1}^m \subset \mathcal{D}_s$  do
3:      $\mathcal{L}_{cls}(\theta) = \frac{1}{m} \sum_{i=1}^m \ell(y_i, \hat{f}(\mathbf{x}_i, \theta))$ 
4:     Initialize  $\mathcal{L}_{inv}(\theta) = 0$  and  $\mathcal{B}' = []$ 
5:     for each  $(\mathbf{x}_i, z_i, y_i)$  in the minibatch do
6:       Generate  $(\mathbf{x}_j, z_j, y_j) = \text{DATAAUG}(\mathbf{x}_i, z_i, y_i)$  and add it to  $\mathcal{B}'$ 
7:        $\mathcal{L}_{inv}(\theta) += \frac{1}{m} d[\hat{f}(\mathbf{x}_i, \theta), \hat{f}(\mathbf{x}_j, \theta)]$ 
8:     end for
9:      $\mathcal{L}_{fair}(\theta) = \left| \frac{1}{m} \sum_{(\mathbf{x}_i, z_i) \in \mathcal{B}} g(\hat{f}(\mathbf{x}_i, \theta), z_i) \right| + \left| \frac{1}{m} \sum_{(\mathbf{x}_j, z_j) \in \mathcal{B}'} g(\hat{f}(\mathbf{x}_j, \theta), z_j) \right|$ 
10:     $\mathcal{L}(\theta) = \mathcal{L}_{cls}(\theta) + \lambda_1 \cdot \mathcal{L}_{inv}(\theta) + \lambda_2 \cdot \mathcal{L}_{fair}(\theta)$ 
11:     $\theta \leftarrow \text{Adam}(\mathcal{L}(\theta), \theta, \eta_p)$ 
12:     $\lambda_1 \leftarrow \max\{\lambda_1 + \eta_d \cdot (\mathcal{L}_{inv}(\theta) - \gamma_1), 0\}$ ,  $\lambda_2 \leftarrow \max\{\lambda_2 + \eta_d \cdot (\mathcal{L}_{fair}(\theta) - \gamma_2), 0\}$ 
13:  end for
14: until convergence
15: procedure DATAAUG( $\mathbf{x}, z, y$ )
16:    $\mathbf{c}, \mathbf{a}, \mathbf{s} = E(\mathbf{x})$ 
17:   Sample  $\mathbf{a}' \sim \mathcal{N}(0, I_a)$ ,  $\mathbf{s}' \sim \mathcal{N}(0, I_s)$ 
18:    $\mathbf{x}' = G(\mathbf{c}, \mathbf{a}', \mathbf{s}')$ ,  $z' = h(\mathbf{a}')$ 
19:   return  $(\mathbf{x}', z', y)$ 
20: end procedure
```

Table 1: Statistics summary of all datasets.

Dataset	Domain, e	Sensitive label, Z	Class label, Y	$(e, \rho^e), \forall e \in \mathcal{E}$
ccMNIST	digit color	background color	digit label	(R, 0.11), (G, 0.43), (B, 0.87)
FairFace	race	gender	age	(B, 0.91), (E, 0.87), (I, 0.58), (L, 0.48), (M, 0.87), (S, 0.39), (W, 0.49)
YFCC100M-FDG	year	location	indoor/outdoor	$(d_0, 0.73)$, $(d_1, 0.84)$, $(d_2, 0.72)$
NYSF	city	race	stop record	(R, 0.93), (B, 0.85), (M, 0.81), (Q, 0.98), (S, 0.88)

5 Experiments

Settings. We evaluate the performance of our FDDG on four benchmarks. To highlight each domain e and its fair dependence score ρ^e , we summarize the statistic in Tab. 1. Three image datasets ccMNIST, FairFace [21], YFCC100M-FDG [22], and one tabular dataset New York Stop-and-Frisk (NYSF) [23] are conducted on FDDG against 17 state-of-the-art baseline methods that fall into two categories, state-of-the-art DG methods (RandAug¹, ERM [24], IRM [8], GDRO [25], Mixup [26], MLDG [27], CORAL [28], MMD [29], DANN [30], CDANN [31], DDG [13], and MBDG [12]) and fairness-aware methods in changing environments (DDG-FC, MBDG-FC², EIIL [4], FarconVAE [5], FATDM [6]). Three metrics are used for evaluation. Two of them are for fairness quantification, Demographic Parity (DP) [14] and the Area Under the ROC Curve (AUC) between predictions of sensitive subgroups [32]. Notice that the AUC metric is not the same as the one commonly used in classification based on TPR and FPR. The intuition behind this AUC is based on the nonparametric *Mann-Whitney U* test, in which a fair condition is defined as the probability of a randomly selected sample \mathbf{x}_{-1} from one sensitive subgroup being greater than a randomly selected sample \mathbf{x}_1 from the other sensitive subgroup is equal to the probability of \mathbf{x}_1 being greater than \mathbf{x}_{-1} [33, 34]. A value of DP closer to 1 indicates fairness and 0.5 of AUC represents zero bias effect on predictions. Due to space limits, we defer a detailed description of the experimental settings (including datasets, baselines, evaluation metrics, etc.) in Appendix C and complete results on all baselines and datasets in Appendix F.

Data Reconstruction and Generation via T . To assess the effectiveness of the transformation model T , we visualize instance reconstruction and domain variation using image datasets in Fig. 3. The first column (Original) shows the images sampled from the datasets. In the second column (Reconstruction), we display images that are generated from latent factors encoded from the images in the first column. The images in the second column closely resemble those in

¹RandAug (or ColorJitter) is a naive built-in function in *Torch* used for image transformations. It randomly changes the brightness, contrast, saturation, and hue of given images.

²DDG-FC and MBDG-FC are two fairness-aware DG baselines that built upon DDG [13] and MBDG [12], respectively. These extensions involve the straightforward addition of fairness constraints defined in Defn. 1 to the loss functions of the original models.

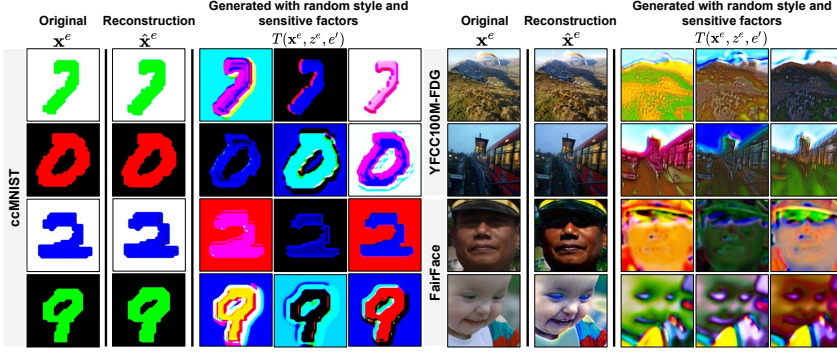


Figure 3: Visualizations for images under reconstruction and the transformation model T with random style and sensitive factors.

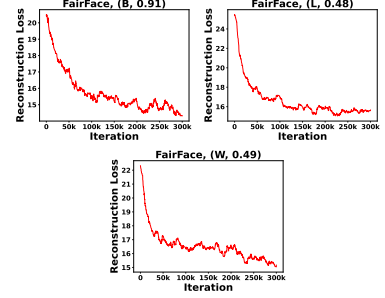


Figure 4: Tracking the change of reconstruction loss using the B/L/W domains of the FairFace dataset.

Table 2: Performance on for FairFace. **Bold** is the best and underline is the second best.

Methods	DP \uparrow / AUC \downarrow / Accuracy \uparrow			
	(B, 0.91)	(L, 0.48)	(W, 0.49)	Avg
RandAug	$0.64 \pm 0.26 / 0.64 \pm 0.15 / 93.47 \pm 1.56$	$0.39 \pm 0.10 / 0.70 \pm 0.02 / 91.77 \pm 0.61$	$0.34 \pm 0.09 / 0.64 \pm 0.02 / 92.07 \pm 0.55$	$0.42 / 0.66 / 92.94$
ERM	$0.67 \pm 0.17 / 0.58 \pm 0.02 / 91.89 \pm 1.10$	$0.57 \pm 0.15 / 0.62 \pm 0.01 / 91.96 \pm 0.51$	$0.39 \pm 0.09 / 0.61 \pm 0.01 / 92.82 \pm 0.38$	$0.51 / 0.61 / 93.08$
IRM	$0.63 \pm 0.12 / 0.58 \pm 0.01 / 93.39 \pm 1.03$	$0.41 \pm 0.21 / 0.63 \pm 0.05 / 92.06 \pm 1.89$	$0.32 \pm 0.19 / 0.66 \pm 0.01 / 90.54 \pm 1.56$	$0.43 / 0.62 / 92.48$
GDRO	$0.71 \pm 0.16 / 0.57 \pm 0.02 / 89.81 \pm 1.10$	$0.54 \pm 0.15 / 0.62 \pm 0.01 / 91.59 \pm 0.51$	$0.48 \pm 0.09 / 0.60 \pm 0.01 / 92.50 \pm 0.38$	$0.55 / 0.60 / 92.55$
Mixup	$0.58 \pm 0.19 / 0.59 \pm 0.02 / 92.46 \pm 0.69$	$0.55 \pm 0.22 / 0.61 \pm 0.02 / 93.43 \pm 2.02$	$0.43 \pm 0.19 / 0.61 \pm 0.01 / 92.98 \pm 0.03$	$0.51 / 0.60 / 93.19$
DDG	$0.60 \pm 0.20 / 0.59 \pm 0.02 / 91.76 \pm 1.03$	$0.44 \pm 0.17 / 0.62 \pm 0.02 / 93.46 \pm 0.32$	$0.51 \pm 0.07 / 0.60 \pm 0.01 / 91.34 \pm 0.80$	$0.49 / 0.61 / 92.74$
MBDG	$0.60 \pm 0.15 / 0.58 \pm 0.01 / 91.29 \pm 1.41$	$0.56 \pm 0.09 / 0.61 \pm 0.01 / 93.49 \pm 0.97$	$0.30 \pm 0.04 / 0.62 \pm 0.01 / 91.05 \pm 0.53$	$0.50 / 0.60 / 92.71$
DDG-FC	$0.61 \pm 0.06 / 0.58 \pm 0.03 / 92.27 \pm 1.65$	$0.50 \pm 0.25 / 0.62 \pm 0.03 / 92.42 \pm 0.30$	$0.48 \pm 0.15 / 0.62 \pm 0.02 / 92.45 \pm 1.55$	$0.52 / 0.61 / 93.23$
MBDG-FC	$0.70 \pm 0.15 / 0.56 \pm 0.03 / 92.12 \pm 0.43$	$0.57 \pm 0.23 / 0.62 \pm 0.02 / 91.89 \pm 0.81$	$0.32 \pm 0.07 / 0.60 \pm 0.03 / 91.50 \pm 0.57$	$0.53 / 0.60 / 92.48$
EIIL	$0.88 \pm 0.07 / 0.59 \pm 0.05 / 84.75 \pm 2.16$	$0.49 \pm 0.07 / 0.59 \pm 0.01 / 88.39 \pm 1.25$	$0.46 \pm 0.05 / 0.65 \pm 0.03 / 86.53 \pm 1.02$	$0.64 / 0.61 / 87.78$
FarconVAE	$0.93 \pm 0.03 / 0.54 \pm 0.01 / 89.61 \pm 0.64$	0.58 $\pm 0.05 / 0.60 \pm 0.05 / 88.70 \pm 0.71$	$0.51 \pm 0.07 / 0.60 \pm 0.01 / 86.40 \pm 0.42$	$0.66 / 0.58 / 88.46$
FATDM	$0.93 \pm 0.03 / 0.57 \pm 0.02 / 92.20 \pm 0.36$	$0.51 \pm 0.16 / 0.63 \pm 0.02 / 93.33 \pm 0.20$	$0.46 \pm 0.05 / 0.63 \pm 0.01 / 92.56 \pm 0.31$	$0.67 / 0.61 / 92.54$
FDDG	0.94 $\pm 0.05 / 0.55 \pm 0.02 / 93.91 \pm 0.33$	0.58 $\pm 0.15 / 0.59 \pm 0.01 / 93.73 \pm 0.26$	0.52 $\pm 0.17 / 0.58 \pm 0.03 / 93.02 \pm 0.50$	0.70 / 0.58 / 93.42

the first column. We showcase the reconstruction loss using the FairFace dataset in Fig. 4. Images in the last three columns are generated using the content factors that were encoded from images in the first column. These images are generated with style and sensitive factors randomly sampled from their respective prior distributions. The images in the last three columns preserve the underlying semantic information of the corresponding samples in the first column. However, their style and sensitive attributes undergo significant changes. This demonstrates that the transformation model T effectively extracts latent factors and produces diverse transformations of the provided data domains. More visualization and plot results are given in Appendix F.

The Effectiveness of FDDG Across Domains in terms of Fairness and Accuracy. Comprehensive experiments showcase that FDDG consistently outperforms baselines by a considerable margin. For all tables in the main paper and Appendix, results shown in each column represent performance on the target domain, using the rest as source domains. Due to space limit, selected results for three domains of FairFace are shown in Tab. 2, but the average results are based on all domains. Complete performance for all domains of datasets refers to Appendix F. As shown in Tab. 2, for the FairFace dataset, our method has the best accuracy and fairness level for the average DG performance over all the domains. More specifically, our method has better fairness metrics (4% for DP, 2% for AUC) and comparable accuracy (0.23% better) than the best of the baselines for individual metrics. As shown in Tab. 3, for YFCC100M-FDG, our method excels in fairness metrics (8% for DP, 5% for AUC) and comparable accuracy (0.35% better) compared to the best baselines.

Ablation Studies. We conduct three ablation studies to study the robustness of FDDG on FairFace. In-depth descriptions and the pseudocodes for these studies can be found in Appendix D. More results can be found in Appendix F. (1) In FDDG w/o sf, we modify the encoder within T by restricting its output to only latent content and style factors. (2) FDDG w/o T skips data augmentation in synthetic domains via T and results are conducted only based f constrained by fair notions outlined in Defn. 1. (3) In FDDG w/o fc, the fair constraint on f is not included, and we eliminate the \mathcal{L}_{fair} in line 9 of Algorithm 1. We include the performance of such ablation studies in Tab. 4. The results illustrate that when data is disentangled into three factors and the model is designed accordingly, it can enhance DG performance due to covariate and dependence shifts. Generating data in synthetic domains with randomly fair dependence patterns proves to be an effective approach for ensuring fairness invariance across domains.

Table 3: Performance on YFCC100M-FDG. (bold is the best; underline is the second best).

Methods	DP \uparrow / AUC \downarrow / Accuracy \uparrow			
	(d_0 , 0.73)	(d_1 , 0.84)	(d_2 , 0.72)	Avg
RandAug	0.67 \pm 0.06 / 0.57 \pm 0.02 / 57.47 \pm 1.20	0.67 \pm 0.34 / 0.61 \pm 0.01 / 82.43 \pm 1.25	0.65 \pm 0.21 / 0.64 \pm 0.02 / 87.88 \pm 0.35	0.66 / 0.61 / 75.93
ERM	0.81 \pm 0.09 / 0.58 \pm 0.01 / 40.51 \pm 0.23	0.71 \pm 0.18 / 0.66 \pm 0.03 / 83.91 \pm 0.33	0.89 \pm 0.08 / 0.59 \pm 0.01 / 82.06 \pm 0.33	0.80 / 0.61 / 68.83
IRM	0.76 \pm 0.10 / 0.58 \pm 0.02 / 50.51 \pm 2.44	0.87 \pm 0.08 / 0.60 \pm 0.02 / 73.26 \pm 0.03	0.70 \pm 0.24 / 0.57 \pm 0.02 / 82.78 \pm 2.19	0.78 / 0.58 / 68.85
GDRO	0.80 \pm 0.05 / 0.59 \pm 0.01 / 53.43 \pm 2.29	0.73 \pm 0.22 / 0.60 \pm 0.01 / 87.56 \pm 2.20	0.79 \pm 0.13 / 0.65 \pm 0.02 / 83.10 \pm 0.64	0.78 / 0.62 / 74.70
Mixup	0.82 \pm 0.07 / 0.57 \pm 0.03 / 61.15 \pm 0.28	0.79 \pm 0.14 / 0.63 \pm 0.03 / 78.63 \pm 0.97	0.89 \pm 0.05 / 0.60 \pm 0.01 / 85.18 \pm 0.80	0.84 / 0.60 / 74.99
DDG	0.81 \pm 0.14 / 0.57 \pm 0.03 / 60.08 \pm 1.08	0.74 \pm 0.12 / 0.66 \pm 0.03 / 92.53 \pm 0.91	0.71 \pm 0.21 / 0.59 \pm 0.03 / 95.02 \pm 1.92	0.75 / 0.61 / 82.54
MBDG	0.79 \pm 0.15 / 0.58 \pm 0.01 / 60.46 \pm 1.90	0.73 \pm 0.07 / 0.67 \pm 0.01 / 94.36 \pm 0.23	0.71 \pm 0.11 / 0.59 \pm 0.03 / <u>93.48</u> \pm 0.65	0.74 / 0.61 / <u>82.77</u>
DDG-FC	0.76 \pm 0.06 / 0.58 \pm 0.03 / 59.96 \pm 2.36	0.83 \pm 0.06 / 0.58 \pm 0.01 / 96.80 \pm 1.28	0.82 \pm 0.09 / 0.59 \pm 0.01 / 86.38 \pm 2.45	0.80 / 0.58 / 81.04
MBDG-FC	0.80 \pm 0.13 / 0.58 \pm 0.01 / <u>62.31</u> \pm 0.13	0.72 \pm 0.09 / 0.63 \pm 0.01 / <u>94.73</u> \pm 2.09	0.80 \pm 0.07 / 0.53 \pm 0.01 / 87.78 \pm 2.11	0.77 / 0.58 / 81.61
EIIL	0.87 \pm 0.11 / 0.55 \pm 0.02 / 56.74 \pm 0.60	0.76 \pm 0.05 / 0.54 \pm 0.03 / 68.99 \pm 0.91	0.87 \pm 0.06 / 0.78 \pm 0.03 / 72.19 \pm 0.75	0.83 / 0.62 / 65.98
FarconVAE	0.67 \pm 0.06 / 0.61 \pm 0.03 / 51.21 \pm 0.61	0.90 \pm 0.06 / 0.59 \pm 0.01 / 72.40 \pm 2.13	0.85 \pm 0.12 / 0.55 \pm 0.01 / 74.20 \pm 2.46	0.81 / 0.58 / 65.93
FATDM	0.80 \pm 0.10 / <u>0.55</u> \pm 0.03 / 61.56 \pm 0.89	0.88 \pm 0.08 / 0.56 \pm 0.01 / 90.00 \pm 0.66	0.86 \pm 0.10 / 0.60 \pm 0.02 / 89.12 \pm 1.30	<u>0.84</u> / <u>0.57</u> / 80.22
FDDG	0.87 \pm 0.09 / 0.53 \pm 0.01 / 62.56 \pm 2.25	0.94 \pm 0.05 / 0.52 \pm 0.01 / 93.36 \pm 1.70	0.93 \pm 0.03 / 0.53 \pm 0.02 / 93.43 \pm 0.73	0.92 / 0.53 / 83.12

Table 4: Ablation studies results on FairFace.

Methods	DP \uparrow / AUC \downarrow / Accuracy \uparrow			
	(B, 0.91)	(L, 0.48)	(W, 0.49)	Avg
FDDG w/o sf	0.68 \pm 0.18 / 0.57 \pm 0.02 / 93.07 \pm 0.68	0.47 \pm 0.07 / 0.63 \pm 0.01 / 92.62 \pm 0.93	0.35 \pm 0.26 / 0.58 \pm 0.01 / 92.18 \pm 0.46	0.49 / 0.59 / 93.08
FDDG w/o T	0.83 \pm 0.08 / 0.56 \pm 0.01 / 92.81 \pm 0.81	0.53 \pm 0.03 / 0.59 \pm 0.01 / 91.19 \pm 0.57	0.52 \pm 0.23 / 0.59 \pm 0.01 / 90.78 \pm 0.31	0.58 / 0.59 / 91.65
FDDG w/o fc	0.59 \pm 0.16 / 0.58 \pm 0.01 / 92.92 \pm 1.35	0.40 \pm 0.07 / 0.70 \pm 0.02 / 92.96 \pm 0.85	0.34 \pm 0.08 / 0.72 \pm 0.03 / 91.88 \pm 0.67	0.42 / 0.66 / 93.01

6 Conclusion

Differing from established domain generalization research, which attributes distribution shifts from source domains to target domains to concept shift and covariate shift, we introduce a novel form of distribution shift known as dependence shift. This shift pertains to varying dependence patterns between model outcomes and sensitive attributes in different domains. Furthermore, we introduce a novel approach to fairness-aware learning designed to tackle the challenges of domain generalization when confronted with both covariate shift and dependence shift simultaneously. In our pursuit of learning a fairness-aware invariant classifier across domains, we assert the existence of an underlying transformation model that can transform instances from one domain to another. This model plays a crucial role in achieving fairness-aware domain generalization by generating instances in synthetic domains characterized by novel data styles and fair dependence patterns. We present a practical and tractable algorithm, accompanied by comprehensive theoretical analyses and exhaustive empirical studies. We showcase the algorithm’s effectiveness through rigorous comparisons with state-of-the-art baselines.

References

- [1] Richard Zemel, Yu Wu, Kevin Swersky, Toniann Pitassi, and Cynthia Dwork. Learning fair representations. *ICML*, 2013.
- [2] Chen Zhao, Feng Chen, and Bhavani Thuraisingham. Fairness-aware online meta-learning. *ACM SIGKDD*, 2021.
- [3] Yongkai Wu, Lu Zhang, and Xintao Wu. On convexity and bounds of fairness-aware classification. 2019.
- [4] Elliot Creager, Jörn-Henrik Jacobsen, and Richard Zemel. Environment inference for invariant learning. In *International Conference on Machine Learning*, pages 2189–2200. PMLR, 2021.
- [5] Changdae Oh, Heeji Won, Junhyuk So, Taero Kim, Yewon Kim, Hosik Choi, and Kyungwoo Song. Learning fair representation via distributional contrastive disentanglement. In *Proceedings of the 28th ACM SIGKDD Conference on Knowledge Discovery and Data Mining*, pages 1295–1305, 2022.
- [6] Thai-Hoang Pham, Xueru Zhang, and Ping Zhang. Fairness and accuracy under domain generalization. *Proceedings of the International Conference on Learning Representations*, 2023.
- [7] Jose G Moreno-Torres, Troy Raeder, Rocío Alaiz-Rodríguez, Nitesh V Chawla, and Francisco Herrera. A unifying view on dataset shift in classification. *Pattern recognition*, 45(1):521–530, 2012.
- [8] Martin Arjovsky, Léon Bottou, Ishaan Gulrajani, and David Lopez-Paz. Invariant risk minimization. *arXiv preprint arXiv:1907.02893*, 2019.

- [9] Beidi Chen, Weiyang Liu, Zhiding Yu, Jan Kautz, Anshumali Shrivastava, Animesh Garg, and Animashree Anandkumar. Angular visual hardness. In *International Conference on Machine Learning*, pages 1637–1648. PMLR, 2020.
- [10] David Krueger, Ethan Caballero, Joern-Henrik Jacobsen, Amy Zhang, Jonathan Binas, Dinghui Zhang, Remi Le Priol, and Aaron Courville. Out-of-distribution generalization via risk extrapolation (rex). In *International Conference on Machine Learning*, pages 5815–5826. PMLR, 2021.
- [11] Chaochao Lu, Yuhuai Wu, José Miguel Hernández-Lobato, and Bernhard Schölkopf. Nonlinear invariant risk minimization: A causal approach. *arXiv preprint arXiv:2102.12353*, 2021.
- [12] Alexander Robey, George J Pappas, and Hamed Hassani. Model-based domain generalization. *Advances in Neural Information Processing Systems*, 34:20210–20229, 2021.
- [13] Hanlin Zhang, Yi-Fan Zhang, Weiyang Liu, Adrian Weller, Bernhard Schölkopf, and Eric P Xing. Towards principled disentanglement for domain generalization. In *Proceedings of the IEEE/CVF Conference on Computer Vision and Pattern Recognition*, pages 8024–8034, 2022.
- [14] Cynthia Dwork, Moritz Hardt, Toniann Pitassi, Omer Reingold, and Rich Zemel. Fairness through awareness. *CoRR*, 2011.
- [15] Michael Lohaus, Michael Perrot, and Ulrike Von Luxburg. Too relaxed to be fair. In *ICML*, 2020.
- [16] Chen Zhao, Feng Mi, Xintao Wu, Kai Jiang, Latifur Khan, Christan Grant, and Feng Chen. Towards fair disentangled online learning for changing environments. In *Proceedings of the 29th ACM SIGKDD Conference on Knowledge Discovery and Data Mining*, pages 3480–3491, 2023.
- [17] Yujie Lin, Chen Zhao, Minglai Shao, Baoluo Meng, Xujiang Zhao, and Haifeng Chen. Pursuing counterfactual fairness via sequential autoencoder across domains. *ArXiv:2309.13005*, 2023.
- [18] Xun Huang, Ming-Yu Liu, Serge Belongie, and Jan Kautz. Multimodal unsupervised image-to-image translation. In *Proceedings of the European conference on computer vision (ECCV)*, pages 172–189, 2018.
- [19] Ming-Yu Liu, Thomas Breuel, and Jan Kautz. Unsupervised image-to-image translation networks. *Advances in neural information processing systems*, 30, 2017.
- [20] Dominik Maria Endres and Johannes E Schindelin. A new metric for probability distributions. *IEEE Transactions on Information theory*, 49(7):1858–1860, 2003.
- [21] Kimmo Karkkainen and Jungseock Joo. Fairface: Face attribute dataset for balanced race, gender, and age for bias measurement and mitigation. In *Proceedings of the IEEE/CVF Winter Conference on Applications of Computer Vision (WACV)*, pages 1548–1558, January 2021.
- [22] Bart Thomee, David A Shamma, Gerald Friedland, Benjamin Elizalde, Karl Ni, Douglas Poland, Damian Borth, and Li-Jia Li. Yfcc100m: The new data in multimedia research. *Communications of the ACM*, 59(2):64–73, 2016.
- [23] Pang Wei Koh, Shiori Sagawa, Henrik Marklund, Sang Michael Xie, Marvin Zhang, Akshay Balsubramani, Weihua Hu, Michihiro Yasunaga, Richard Lanus Phillips, Irena Gao, Tony Lee, Etienne David, Ian Stavness, Wei Guo, Berton Earnshaw, Imran Haque, Sara M Beery, Jure Leskovec, Anshul Kundaje, Emma Pierson, Sergey Levine, Chelsea Finn, and Percy Liang. Wilds: A benchmark of in-the-wild distribution shifts. In *ICML*, 2021.
- [24] Vladimir Vapnik. *The nature of statistical learning theory*. Springer science & business media, 1999.
- [25] Shiori Sagawa, Pang Wei Koh, Tatsunori B Hashimoto, and Percy Liang. Distributionally robust neural networks. *International Conference on Learning Representations*, 2020.
- [26] Shen Yan, Huan Song, Nanxiang Li, Lincan Zou, and Liu Ren. Improve unsupervised domain adaptation with mixup training. *arXiv preprint arXiv:2001.00677*, 2020.
- [27] Da Li, Yongxin Yang, Yi-Zhe Song, and Timothy Hospedales. Learning to generalize: Meta-learning for domain generalization. In *Proceedings of the AAAI conference on artificial intelligence*, volume 32, 2018.
- [28] Baochen Sun and Kate Saenko. Deep coral: Correlation alignment for deep domain adaptation. In *European conference on computer vision*, pages 443–450. Springer, 2016.
- [29] Haoliang Li, Sinno Jialin Pan, Shiqi Wang, and Alex C Kot. Domain generalization with adversarial feature learning. In *Proceedings of the IEEE conference on computer vision and pattern recognition*, pages 5400–5409, 2018.
- [30] Yaroslav Ganin, Evgeniya Ustinova, Hana Ajakan, Pascal Germain, Hugo Larochelle, François Laviolette, Mario Marchand, and Victor Lempitsky. Domain-adversarial training of neural networks. *The journal of machine learning research*, 17(1):2096–2030, 2016.

- [31] Ya Li, Xinmei Tian, Mingming Gong, Yajing Liu, Tongliang Liu, Kun Zhang, and Dacheng Tao. Deep domain generalization via conditional invariant adversarial networks. In *Proceedings of the European Conference on Computer Vision (ECCV)*, pages 624–639, 2018.
- [32] Charles X Ling, Jin Huang, Harry Zhang, et al. Auc: a statistically consistent and more discriminating measure than accuracy. In *Ijcai*, volume 3, pages 519–524, 2003.
- [33] Chen Zhao and Feng Chen. Rank-based multi-task learning for fair regression. *IEEE International Conference on Data Mining (ICDM)*, 2019.
- [34] Toon Calders, Asim Karim, Faisal Kamiran, Wasif Ali, and Xiangliang Zhang. Controlling attribute effect in linear regression. *ICDM*, 2013.
- [35] Riccardo Volpi, Diane Larlus, and Grégory Rogez. Continual adaptation of visual representations via domain randomization and meta-learning. In *Proceedings of the IEEE/CVF Conference on Computer Vision and Pattern Recognition*, pages 4443–4453, 2021.
- [36] Kaiyang Zhou, Yongxin Yang, Timothy Hospedales, and Tao Xiang. Learning to generate novel domains for domain generalization. In *Computer Vision–ECCV 2020: 16th European Conference, Glasgow, UK, August 23–28, 2020, Proceedings, Part XVI 16*, pages 561–578. Springer, 2020.
- [37] Gilles Blanchard, Gyemin Lee, and Clayton Scott. Generalizing from several related classification tasks to a new unlabeled sample. *Advances in neural information processing systems*, 24, 2011.
- [38] Gill Kirton. Unions and equality: 50 years on from the fight for fair pay at dagenham. *Employee Relations: The International Journal*, 41(2):344–356, 2019.
- [39] Sergio Alonso, Rosana Montes, Daniel Molina, Iván Palomares, Eugenio Martínez-Cámara, Manuel Chiachio, Juan Chiachio, Francisco J Melero, Pablo García-Moral, Bárbara Fernández, et al. Ordering artificial intelligence based recommendations to tackle the sdgs with a decision-making model based on surveys. *Sustainability*, 13(11):6038, 2021.
- [40] Ashkan Rezaei, Anqi Liu, Omid Memarrast, and Brian D Ziebart. Robust fairness under covariate shift. In *Proceedings of the AAAI Conference on Artificial Intelligence*, volume 35, pages 9419–9427, 2021.
- [41] Harvineet Singh, Rina Singh, Vishwali Mhasawade, and Rumi Chunara. Fairness violations and mitigation under covariate shift. In *Proceedings of the 2021 ACM Conference on Fairness, Accountability, and Transparency*, pages 3–13, 2021.
- [42] Stephen Giguere, Blossom Metevier, Yuriy Brun, Bruno Castro da Silva, Philip S Thomas, and Scott Niekum. Fairness guarantees under demographic shift. In *Proceedings of the 10th International Conference on Learning Representations (ICLR)*, 2022.
- [43] Yatong Chen, Reilly Raab, Jialu Wang, and Yang Liu. Fairness transferability subject to bounded distribution shift. *Advances in Neural Information Processing Systems*, 35:11266–11278, 2022.
- [44] Yann LeCun, Léon Bottou, Yoshua Bengio, and Patrick Haffner. Gradient-based learning applied to document recognition. *Proceedings of the IEEE*, 86(11):2278–2324, 1998.
- [45] Michael Feldman, Sorelle Friedler, John Moeller, Carlos Scheidegger, and Suresh Venkatasubramanian. Certifying and removing disparate impact. *KDD*, 2015.
- [46] Ian Goodfellow, Jean Pouget-Abadie, Mehdi Mirza, Bing Xu, David Warde-Farley, Sherjil Ozair, Aaron Courville, and Yoshua Bengio. Generative adversarial networks. *Communications of the ACM*, 63(11):139–144, 2020.
- [47] Kaiming He, Xiangyu Zhang, Shaoqing Ren, and Jian Sun. Deep residual learning for image recognition. In *Proceedings of the IEEE conference on computer vision and pattern recognition*, pages 770–778, 2016.
- [48] Ishaan Gulrajani and David Lopez-Paz. In search of lost domain generalization. *arXiv preprint arXiv:2007.01434*, 2020.

Supplementary Materials

A Related Works

Domain generalization. Addressing the challenge of domain shift and the absence of OOD data has led to the introduction of several state-of-the-art methods in the domain generalization field [24, 8, 13, 12]. These methods are designed to enable deep learning models to possess intrinsic generalizability, allowing them to adapt effectively from one or multiple source domains to target domains characterized by unknown distributions [35]. They encompass various techniques, such as aligning source domain distributions to facilitate domain-invariant representation learning [29], subjecting the model to domain shift during training through meta-learning [27], and augmenting data with domain analysis, among others [36], and so on. In the context of the number of source domains, a significant portion of research [13, 12, 37] has focused on the multi-source setting. This setting assumes the availability of multiple distinct but relevant domains for the generalization task. As mentioned in [37], the primary motivation for studying domain generalization is to harness data from multiple sources in order to unveil stable patterns. This entails learning representations that are invariant to the marginal distributions of data features, all while lacking access to the target data. Nevertheless, existing domain generalization methods tend to overlook the aspect of learning with fairness, where group fairness dependence patterns may not undergo changes across domains.

Fairness learning for changing environments. Two primary research directions aim to tackle fairness-aware machine learning in dynamic or changing environments. The first approach involves equality-aware monitoring methods [38, 39, 6, 40, 41, 42, 43], which strive to identify and mitigate unfairness in a model’s behavior by continuously monitoring its predictions. These methods adapt the model’s parameters or structure when unfairness is detected. However, a significant limitation of such approaches is their assumption of invariant fairness levels across domains, which may not hold in real-world applications. The second approach [5, 4] focuses on evaluating a model’s fairness in a dynamic environment by treating shifted fairness levels as domain labels. However, it does not take into account distribution shifts in non-sensitive features.

In response to these limitations, this paper adopts a novel approach by attributing the distribution shift from source to target domains to both covariate shift and fairness dependence shift simultaneously. We aim to train a fairness-aware invariant classifier that can generalize effectively across domains, ensuring robust performance in terms of both model accuracy and maintaining fair dependence between predicted outcomes and sensitive attributes even under these shifts.

B Notations

For clear interpretation, we list the notations used in this paper and their corresponding explanation, as shown in Tab. 5.

C Experimental Settings

C.1 Datasets.

We consider four datasets: ccMNIST, FairFace, YFCC100M-FDG, and New York Stop-and-Frisk (NYSF) to evaluate our FDDG against state-of-the-art baseline methods, where NYSF is a tabular data and the other three are image datasets.

(a) ccMNIST is a domain generalization benchmark created by colorizing digits and the backgrounds of the MNIST dataset [44]. ccMNIST consists of images of handwritten digits from 0 to 9. Similar to ColoredMNIST [8], for binary classification, digits are labeled with 0 and 1 for digits from 0-4 and 5-9, respectively. ccMNIST contains three data domains, each characterized by a different digit color (*i.e.*, red, green, blue) with 70,000 images. Each image has a black or white background color as the sensitive label. The domains are constructed so that each domain has a different correlation between the class label and sensitive attribute (digit background colors), specifically 0.9 for the red domain, 0.7 for the green domain, and 0 for the blue domain.

(b) FairFace [21] is a dataset that contains a balanced representation of different racial groups. It includes 108,501 images from seven racial categories: Black (B), East Asian (E), Indian (I), Latino (L), Middle Eastern (M), Southeast Asian (S), and White (W). In our experiments, we set each racial group as a domain, gender as the sensitive label, and age (\geq or $<$ 50) as the class label.

(c) YFCC100M-FDG is an image dataset created by *Yahoo Labs* and released to the public in 2014. It is randomly selected from the YFCC100M [22] dataset with a total of 90,000 images. For domain variations, YFCC100M-FDG is divided into three domains. Each contains 30,000 images from different year ranges, before 1999 (d_0), 2000 to 2009

Table 5: Important notations and corresponding descriptions.

Notations	Descriptions
\mathcal{X}	input feature space
\mathcal{Z}	sensitive space
\mathcal{Y}	output space
\mathcal{C}	parameterized latent space for content factors
\mathcal{S}	parameterized latent space for style factors
\mathcal{A}	parameterized latent space for sensitive factors
\mathbf{c}	content factor
\mathbf{s}	style factor
\mathbf{a}	sensitive factor
$d[\cdot]$	distance metric on output space
\mathcal{D}	data batch
\mathbf{x}	data features
y	class label
z	sensitive label
f	classifier
\mathcal{F}	model space of classifier
\hat{f}	ξ -parameterization of \mathcal{F}
\hat{y}	predicted class label
Θ	parameter space
$g(Y, Z)$	fairness metric on random variables Y and Z
$ \cdot $	absolute function
p_1	empirical estimate of the proportion of samples in the group $z = 1$
\mathcal{e}	data domain
\mathcal{E}	set of data domains
\mathcal{B}	sampled data batch
T	domain transformation model
E	encoder network
G	decoder network
\mathcal{L}	loss function
δ, ϵ	expectation of the relaxed constraint
h	sensitive label classifier
\hat{z}	sensitive label predicted by h
η_p, η_d	primal and dual learning rate
λ	dual variable
γ	empirical constant

(d_1), and 2010 to 2014 (d_2). The outdoor or Indoor tag is used as the binary class label for each image. Latitude and longitude coordinates, representing where images were taken, are translated into different continents. The continent North-America or non-North-America is used as the sensitive label (related to spatial disparity).

(**d**) NYSF [23] is a real-world dataset on policing in New York City in 2011. It documents whether a pedestrian who was stopped on suspicion of weapon possession would in fact possess a weapon. NYSF consists of records collected in five different sub-cities, Manhattan (M), Brooklyn (B), Queens (Q), Bronx (R), and Staten (S). We use cities as different domains. This data had a pronounced racial bias against African Americans, so we consider race (black or non-black) as the sensitive attribute.

C.2 Baselines.

We compare the performance of our FDDG with 17 baseline methods that fall into three main categories:

- 12 state-of-the-art *domain generalizations* methods (RandAug, ERM [24], IRM [8], GDRO [25], Mixup [26], MLDG [27], CORAL [28], MMD [29], DANN [30], CDANN [31], DDG [13], and MBDG [12]);
- 3 state-of-the-art *fairness-aware learning* methods in changing environments (EIIL [4], FarconVAE [5], and FATDM [6]);

- 2 naive fairness-aware variants of DDG and MBDG, named DDG-FC and MBDG-FC, respectively, by simply adding fairness constraints in Defn. 1 to their classifiers.

Notice that the settings of EIIL and FarconVAE are different from this paper. Both methods characterize domain shift by a different level of correlation between the class label and sensitive features but completely ignore the variation in data features.

C.3 Evaluation Metrics.

Three metrics are used for evaluation, and two of them are for fairness quantification.

- *Demographic Parity* (DP) [14] is formalized as

$$DP = k, \text{ if } DP \leq 1; DP = 1/k, \text{ otherwise, where } k = \mathbb{P}(\hat{Y} = 1|Z = -1)/\mathbb{P}(\hat{Y} = 1|Z = 1)$$

This is also known as a lack of disparate impact [45]. A value closer to 1 indicates fairness.

- *The Area Under the ROC Curve* (AUC) [34] varies from zero to one, and it is symmetric around 0.5, which represents random predictability or zero bias effect on predictions.

$$AUC = \frac{\sum_{(\mathbf{x}_i, z=-1, y_i) \in \mathcal{D}_{-1}} \sum_{(\mathbf{x}_j, z=1, y_j) \in \mathcal{D}_1} I(\mathbb{P}(\hat{y}_i = 1) > \mathbb{P}(\hat{y}_j = 1))}{|\mathcal{D}_{-1}| \times |\mathcal{D}_1|}$$

where $|\mathcal{D}_{-1}|$ and $|\mathcal{D}_1|$ represent sample size of subgroups $z = -1$ and $z = 1$, respectively. $I(\cdot)$ is the indicator function that returns 1 when its argument is true and 0 otherwise.

C.4 Learning the Transformation Model

One goal of the transformation model T is to disentangle an input instance from source domains into three factors in latent spaces by learning a set of encoders $E = \{E^m, E^s, E^c, E^a\}$ and decoders $G = \{G^i, G^o\}$ parameterized by $\{\theta_m, \theta_s, \theta_c, \theta_a\} \in \Theta$ and $\{\phi_i, \phi_o\} \in \Phi$, respectively. As shown in Fig. 5, the learning process of T consists of two levels, an outer level and an inner level, where each level is associated with an auto-encoder system factorizing its corresponding input into two factors within two separated latent spaces. Specifically, in the outer level, an instance is first encoded to a semantic factor $\mathbf{m} \in \mathcal{M}$ and a style factor $\mathbf{s} \in \mathcal{S}$ through the corresponding encoders $E^m : \mathcal{X} \times \Theta \rightarrow \mathcal{M}$ and $E^s : \mathcal{X} \times \Theta \rightarrow \mathcal{S}$, respectively. In the inner level, the semantic factor \mathbf{m} is further encoded to a content factor $\mathbf{c} \in \mathcal{C}$ and a sensitive factor $\mathbf{a} \in \mathcal{A}$, through encoders $E^c : \mathcal{M} \times \Theta \rightarrow \mathcal{C}$ and $E^a : \mathcal{M} \times \Theta \rightarrow \mathcal{A}$. For data reconstruction, two decoders $G^i : \mathcal{C} \times \mathcal{A} \times \Phi \rightarrow \mathcal{M}$ and $G^o : \mathcal{M} \times \mathcal{S} \times \Phi \rightarrow \mathcal{X}$ are introduced in the inner and outer levels. Inspired by image-to-image translation in computer vision [18, 19], our total loss function of learning such encoders and decoders comprises three components: a bidirectional reconstruction loss, a sensitive label prediction loss, and an adversarial loss.

Reconstruction Loss encourages learning reconstruction in two directions: (1) data→latent→data for *data reconstruction*, and (2) latent→data→latent for *factor reconstruction*. For simplicity, we omit parameters for encoders and decoders in the following equations. As for data reconstruction, in terms of the outer and inner levels, an instance \mathbf{x} and its semantic factor \mathbf{m} are required to be reconstructed, respectively.

$$\mathcal{L}_{recon}^{data} = \underbrace{\mathbb{E}_{\mathbf{x} \sim p(\mathbf{x})} [\|G^o(\hat{\mathbf{m}}, E^s(\mathbf{x})) - \mathbf{x}\|_1]}_{\text{data reconstruction}} + \underbrace{\mathbb{E}_{\mathbf{m} \sim p(\mathbf{m})} [\|G^i(E^c(\mathbf{m}), E^a(\mathbf{m})) - \mathbf{m}\|_1]}_{\text{reconstruction of semantic factors } \mathbf{m} \text{ (inner level)}}$$

where $\hat{\mathbf{m}} = G^i(\mathbf{c}, \mathbf{a}) = G^i(E^c(E^m(\mathbf{x})), E^a(E^m(\mathbf{x})))$; $p(\mathbf{m})$ is given by $\mathbf{m} = E^m(\mathbf{x})$ and $\mathbf{x} \sim p(\mathbf{x})$. For factor reconstruction, \mathbf{m} , \mathbf{s} , \mathbf{c} and \mathbf{a} are encouraged to be reconstructed through some latent factors randomly sampled from the prior distributions.

$$\begin{aligned} \mathcal{L}_{recon}^{factor} = & \underbrace{\mathbb{E}_{\mathbf{c} \sim p(\mathbf{c}), \mathbf{a} \sim \mathcal{N}(0, \mathbf{I}_a)} [\|E^c(G^i(\mathbf{c}, \mathbf{a})) - \mathbf{c}\|_1]}_{\text{reconstruction of content factors } \mathbf{c}} + \underbrace{\mathbb{E}_{\mathbf{c} \sim p(\mathbf{c}), \mathbf{a} \sim \mathcal{N}(0, \mathbf{I}_a)} [\|E^a(G^i(\mathbf{c}, \mathbf{a})) - \mathbf{a}\|_1]}_{\text{reconstruction of sensitive factors } \mathbf{a}} \\ & + \underbrace{\mathbb{E}_{\mathbf{m} \sim p(\mathbf{m}), \mathbf{s} \sim \mathcal{N}(0, \mathbf{I}_s)} [\|E^s(G^o(\mathbf{m}, \mathbf{s})) - \mathbf{s}\|_1] + \mathbb{E}_{\mathbf{c} \sim p(\mathbf{c}), \mathbf{s} \sim \mathcal{N}(0, \mathbf{I}_s), \mathbf{a} \sim \mathcal{N}(0, \mathbf{I}_a)} [\|E^s(G^o(G^i(\mathbf{c}, \mathbf{a}), \mathbf{s})) - \mathbf{s}\|_1]}_{\text{reconstruction of style factors } \mathbf{s}} \\ & + \underbrace{\mathbb{E}_{\mathbf{m} \sim p(\mathbf{m}), \mathbf{s} \sim \mathcal{N}(0, \mathbf{I}_s)} [\|E^m(G^o(\mathbf{m}, \mathbf{s})) - \mathbf{m}\|_1]}_{\text{reconstruction of semantic factors } \mathbf{m} \text{ (outer level)}} \end{aligned}$$

where $p(\mathbf{c})$ is given by $\mathbf{c} = E^c(E^m(\mathbf{x}))$, $\mathbf{a} = E^a(E^m(\mathbf{x}))$, and $\mathbf{s} = E^s(\mathbf{x})$.

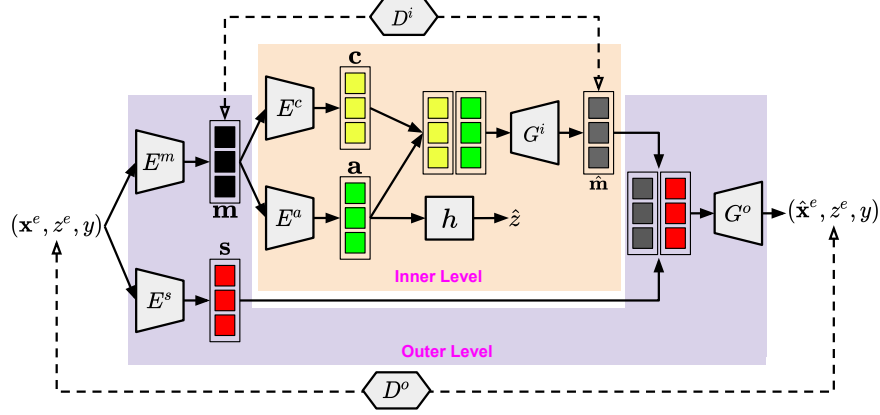


Figure 5: A two-level approach for learning the transformation model T .

Sensitive Loss. Since a sensitive factor is causally dependent on the sensitive features of a datapoint, as shown in the inner level of Fig. 2, a simple classifier $h : \mathcal{A} \times \Theta \rightarrow \mathcal{Z}$ is trained and further it is used to predict the sensitive label using \mathbf{a} in the second stage.

$$\mathcal{L}_{sens} = \text{CrossEntropy}(\mathbf{z}, \hat{\mathbf{z}}) \quad \text{where} \quad \hat{\mathbf{z}} = h(\mathbf{a}, \theta_z) = h(E^a(E^m(\mathbf{x})), \theta_z)$$

Adversarial Loss. Motivated by the observation that GANs [46] can improve data quality for evaluating the disentanglement effect in the latent spaces, we use GANs to match the distribution of reconstructed data to the same distribution. Followed by [18], data and semantic factors generated through encoders and decoders should be indistinguishable from the given ones in the same domain.

$$\begin{aligned} \mathcal{L}_{adv} = & \underbrace{\mathbb{E}_{\mathbf{c} \sim p(\mathbf{c}), \mathbf{s} \sim \mathcal{N}(0, \mathbf{I}_s), \mathbf{a} \sim \mathcal{N}(0, \mathbf{I}_a)} [\log (1 - D^o(G^o(\hat{\mathbf{m}}, \mathbf{s})))] + \mathbb{E}_{\mathbf{x} \sim p(\mathbf{x})} [\log D^o(\mathbf{x})]}_{\text{outer level}} \\ & + \underbrace{\mathbb{E}_{\mathbf{c} \sim p(\mathbf{c}), \mathbf{a} \sim \mathcal{N}(0, \mathbf{I}_a)} [\log (1 - D^i(G^i(\mathbf{c}, \mathbf{a})))] + \mathbb{E}_{\mathbf{m} \sim p(\mathbf{m})} [\log D^i(\mathbf{m})]}_{\text{inner level}} \end{aligned}$$

where $D^o : \mathcal{X} \times \Psi \rightarrow \mathbb{R}$ and $D^i : \mathcal{M} \times \Psi \rightarrow \mathbb{R}$ are the discriminators for the outer and inner levels parameterized by $\psi_o \in \Psi$ and $\psi_i \in \Psi$, respectively.

Total Loss. We jointly train the encoders, decoders, and discriminators to optimize the final objective, a weighted sum of the three loss terms.

$$\min_{E^m, E^s, E^c, E^a, G^i, G^o} \max_{D^i, D^o} \mathcal{L}_{total} = \beta_d \mathcal{L}_{recon}^{data} + \beta_f \mathcal{L}_{recon}^{factor} + \beta_z \mathcal{L}_{sens} + \beta_g \mathcal{L}_{adv} \quad (9)$$

where $\beta_d, \beta_f, \beta_z, \beta_g > 0$ are hyperparameters that control the importance of each loss term. To optimize, the learning algorithm is given in Algorithm 2.

C.5 Architecture Details

We have two sets of networks. One is for ccMNIST, FairFace, and YFCC100M-FDG, and the other one is for the NYSF dataset.

For ccMNIST, FairFace, and YFCC100M-FDG datasets: All the images are resized to 224×224 . E^m and E^c 's structures are the same. Each of them is made of four convolution layers. The first one has 64 filters, and each of the others has 128 filters. The kernel sizes are (7, 7), (4, 4), (3, 3), (3, 3) for layers 1 to 4, respectively. The stride of the second layer is (2, 2), and the stride of all the other layers is (1, 1). The activation function of the first three layers is ReLU. The last convolution layer does not have an activation function. E^s and E^a 's structures are the same. Each of them is made of 6 convolution layers, and there is an adaptive average pooling layer with output size 1 between the last two convolution layers. The numbers of filters are 64, 128, 256, 256, 256, and 2 for the convolution layers, respectively. The kernel sizes are (7, 7), (4, 4), (4, 4), (4, 4), (4, 4), (1, 1). And the strides are (1, 1), (2, 2), (2, 2), (2, 2), (2, 2), (1, 1). The activation function of the first five layers is ReLU. The last convolution layer does not have an activation function. G^o and G^i 's structures are almost the same. The only difference between them is the output size, 3 for G^o and 128

Algorithm 2 Learning the Transformation Model T .

Require: learning rate $\alpha_1, \alpha_2, \alpha_3$, initial coefficients $\beta_d, \beta_f, \beta_z, \beta_g$.

Initialize: Parameter of encoders $\{\theta_m, \theta_s, \theta_c, \theta_a\}$, decoders $\{\phi_i, \phi_o\}$, sensitive classifier θ_z , and discriminators $\{\psi_i, \psi_o\}$.

```
1: repeat
2:   for minibatch  $\{(\mathbf{x}_i, y_i, z_i)\}_{i=1}^q \in \mathcal{D}_s$  do
3:     Compute  $\mathcal{L}_{total}$  for Stage 1 using Eq. (9).
4:      $\psi_o, \psi_i \leftarrow \text{Adam}(\beta_g \mathcal{L}_{adv}, \psi_o, \psi_i, \alpha_1)$ 
5:      $\theta_m, \theta_c, \theta_s, \theta_a, \phi_o, \phi_i \leftarrow \text{Adam}(\beta_d \mathcal{L}_{recon}^{data} + \beta_f \mathcal{L}_{recon}^{factor}, \theta_m, \theta_c, \theta_s, \theta_a, \phi_o, \phi_i, \alpha_2)$ 
6:      $\theta_z \leftarrow \text{Adam}(\beta_z \mathcal{L}_{sens}, \theta_z, \alpha_3)$ 
7:   end for
8: until convergence
9: Return  $\{\theta_m, \theta_s, \theta_c, \theta_a, \theta_z, \phi_i, \phi_o\}$ 
```

for G^i . Each of them has two parts. The first part is made of 4 convolution layers, and there is an upsampling layer with a scale factor 2.0 between the second convolution layer and the third convolution layer. The numbers of filters are 128, 128, 64, and 3 for the convolution layers, respectively. The kernel sizes are (3, 3), (3, 3), (5, 5), (7, 7). The strides are (1, 1) for all the convolution layers. The first and the third convolution layers' activation functions are ReLU. The fourth convolution layer's activation function is Tanh. The second convolution layer does not have an activation function. The second part is made of three fully connected layers. The number of neurons is 256 and 256, respectively, and the output size is 512. The activation function of the first two layers is ReLU, and there is no activation function on the output. D^o comprises 4 convolution layers followed by an average pooling layer whose kernel size is 3, stride is 2, and padding is [1, 1]. The numbers of filters of the convolution layers are 64, 128, 256, 1, respectively. The kernel sizes are (4, 4) for the first three convolution layers and (1, 1) for the fourth convolution layer. The strides are (2, 2) for the first three convolution layers and (1, 1) for the fourth convolution layer. The first three convolution layers' activation functions are LeakyReLU. The other layers do not have activation functions. D^i is made of one fully connected layer whose input size is 112, and the output size is 64 with activation function ReLU. h comprises one fully connected layer with input size 2, output size 1, and activation function Sigmoid. f has two parts. The first part is Resnet-50 [47], and the second is one fully connected layer with input size 2048 and output size 2.

For the NYSF dataset: E^m is made of two fully connected layers. The number of neurons is 32, and the output size is 16. The activation function of the first layer is ReLU, and there is no activation function on the output. E^s is made of two fully connected layers. The number of neurons is 32, and the output size is 2. The activation function of the first layer is ReLU, and there is no activation function on the output. G^o is made of two fully connected layers. The number of neurons is 32, and the output size is 51. The activation function of the first layer is ReLU, and there is no activation function on the output. D^o is made of two fully connected layers. The number of neurons is 32, and the output size is 16. The activation function of the first layer is ReLU, and there is no activation function on the output. E^c is made of two fully connected layers. The number of neurons is 16, and the output size is 8. The activation function of the first layer is ReLU, and there is no activation function on the output. E^a is made of two fully connected layers. The number of neurons is 8, and the output size is 2. The activation function of the first layer is ReLU, and there is no activation function on the output. G^i is made of two fully connected layers. The number of neurons is 16, and the output size is 16. The activation function of the first layer is ReLU, and there is no activation function on the output. D^i is made of two fully connected layers. The number of neurons is 8, and the output size is 8. The activation function of the first layer is ReLU, and there is no activation function on the output. h comprises one fully connected layer with input size 2 and output size 1. The activation function is Sigmoid. f has two parts. The first part is made of 3 fully connected layers. The number of neurons is 32, and the output size is 32. The activation function of the first two layers is ReLU, and there is no activation function on the output. The second part is made of one fully connected layer whose input size is 32, the output size is 32, and it does not have an activation function.

C.6 Hyperparameter Search

We follow the same set of the MUNIT [18] for the hyperparameters. More specifically, the learning rate is 0.0001, the number of iterations is 600000, and the batch size is 1. The loss weights in learning T are chosen from $\{1, 5, 10\}$. The selected best ones are $\beta_d = 10, \beta_f = 1, \beta_z = 1, \beta_g = 1$. We monitor the loss of the validation set and choose the β with the lowest validation loss.

For the hyperparameters in learning the classifier f , the learning rate is chosen from $\{0.000005, 0.00001, 0.00005, 0.0001, 0.0005\}$. η is chosen from $\{0.01, 0.05, 0.1\}$. γ is chosen from $\{0.01, 0.025, 0.05\}$. λ is chosen from $\{0.1, 1, 10, 20\}$. The batch size is chosen from $\{22, 64, 80, 128, 512, 1024, 2048\}$. The numbers of iterations are chosen from $\{500, 1000, \dots, 8000\}$ on the cCMNIST and NYSF datasets. The number of iterations are chosen from $\{300, 600, \dots, 7800, 8000\}$ on the FairFace and YFCC100M-FDG datasets. The selected best ones are: the learning rate is 0.00005, $\eta_1 = \eta_2 = 0.05$, $\gamma_1 = \gamma_2 = 0.025$, $\lambda_1 = \lambda_2 = 1$. The batch size on the cCMNIST and YFCC100M-FDG datasets is 64, and it is 22 on the FairFace dataset and 1024 on the NYSF dataset. The number of iterations on the cCMNIST dataset is 3000, 500, 7000 for domains R, G, B, respectively. The number of iterations on the FairFace dataset is 7200, 7200, 7800, 8000, 6600, 7200, 6900 for domains B, E, I, L, M, S, W, respectively. The number of iterations on the YFCC100M-FDG dataset is 7200, 6000, 6900 for d_0, d_1, d_2 , respectively. The number of iterations on the NYSF dataset is 500, 3500, 4000, 1500, 8000 for domains R, B, M, Q, S, respectively. We monitor the accuracy and the value of fairness metrics from the validation set and select the best ones. The grid space of the grid search on all the baselines is the same as for our method.

C.7 Model Selection.

The model selection in domain generalization is intrinsically a learning problem, followed by [12], we use leave-one-domain-out validation criteria, which is one of the three selection methods stated in [48]. Specifically, we evaluate FDDG on the held-out training domain and average the performance of $|\mathcal{E}_s| - 1$ domains over the held-out one.

D Ablation Studies

We conduct three ablation studies, and detailed algorithms of designed ablation studies are given in Algorithms 3 to 5. For additional ablation study results on cCMNIST, YFCC100M-FDG, and NYSF, refer to Appendix F.

1. The difference between the full FDDG and the first ablation study (FDDG w/o sf) is that the latter does not have the inner level when learning T . Since the inner level is used to extract the content and sensitive factors from the semantic one, the same sensitive label of the generated images will remain due to the absence of $h(\cdot)$. Therefore, FDDG w/o sf is expected to have a lower level of fairness in the experiments. Results shown in the tables indicate that FDDG w/o sf has a significantly lower performance on fairness metrics.
2. The second study (FDDG w/o T) does not train the auto-encoders to generate images. All losses are computed only based on the sampled images. Similar to FDDG w/o sf, it is much harder to train a good classifier without the generated images in synthetic domains. Our results demonstrate that FDDG w/o T performs worse on all the datasets.
3. The difference between FDDG and the third study (FDDG w/o fc) is that FDDG w/o fc does not have the fairness loss \mathcal{L}_{fair} in line 9 of Algorithm 1. Therefore, this algorithm only focuses on accuracy without considering fairness. Results based on FDDG w/o fc show that it has a good level of accuracy but a poor level of fairness.

E Proofs

E.1 Sketch Proof of Theorem 1

Lemma 1. *Given two domains $e_i, e_j \in \mathcal{E}$, $\mathbb{E}_{\mathbb{P}(X^{e_j}, Z^{e_j})} g(f(X^{e_j}), Z^{e_j})$ can be bounded by $\mathbb{E}_{\mathbb{P}(X^{e_i}, Z^{e_i})} g(f(X^{e_i}), Z^{e_i})$ as follows:*

$$\mathbb{E}_{\mathbb{P}(X^{e_j}, Z^{e_j})} g(f(X^{e_j}), Z^{e_j}) \leq \mathbb{E}_{\mathbb{P}(X^{e_i}, Z^{e_i})} g(f(X^{e_i}), Z^{e_i}) + \sqrt{2}D[\mathbb{P}(X^{e_j}, Z^{e_j}, Y^{e_j}), \mathbb{P}(X^{e_i}, Z^{e_i}, Y^{e_i})]$$

Lemma 2. *Given two domains $e_i, e_j \in \mathcal{E}$, under Lemma 1, $\epsilon^{e_j}(f)$ can be bounded by $\epsilon^{e_i}(f)$ as follows:*

$$\epsilon^{e_j}(f) \leq \epsilon^{e_i}(f) + \sqrt{2}D[\mathbb{P}(X^{e_j}, Z^{e_j}, Y^{e_j}), \mathbb{P}(X^{e_i}, Z^{e_i}, Y^{e_i})]$$

Under Lemmas 1 and 2, we now prove Theorem 1

Proof. Let $e_* \in \mathcal{E}_s$ be the source domain nearest to the target domain $e_t \in \mathcal{E} \setminus \mathcal{E}_s$. Under Lemma 2, we have

$$\epsilon^{e_t}(f) \leq \epsilon^{e_*}(f) + \sqrt{2}D[\mathbb{P}(X^{e_t}, Z^{e_t}, Y^{e_t}), \mathbb{P}(X^{e_*}, Z^{e_*}, Y^{e_*})]$$

Algorithm 3 FDDG w/o sf (Ablation Study 1)

```
1: repeat
2:   for minibatch  $\mathcal{B} = \{(\mathbf{x}_i, z_i, y_i)\}_{i=1}^m \in \mathcal{D}_s$  do
3:      $\mathcal{L}_{cls}(\theta) = (1/m) \sum_{i=1}^m \ell(y_i, \hat{f}(\mathbf{x}_i, \theta))$ 
4:      $\mathcal{L}_{fair}(\theta) = (1/m) \sum_{i=1}^m (\frac{1}{p_1(1-p_1)} (\frac{z_i+1}{2} - p_1)) \hat{f}(\mathbf{x}_i, \theta)$ 
5:     for each  $(\mathbf{x}_i, z_i, y_i)$  in the minibatch do
6:        $(\mathbf{x}'_i, z_i, y_i) = \text{DATAAUG}(\mathbf{x}_i, x_i, y_i)$ 
7:        $\mathcal{L}'_{cls}(\theta) = (1/m) \sum_{i=1}^m \ell(y_i, \hat{f}(\mathbf{x}'_i, \theta))$ 
8:     end for
9:      $\mathcal{L}_{cls}(\theta) = \mathcal{L}_{cls}(\theta) + \mathcal{L}'_{cls}(\theta)$ 
10:     $\mathcal{L}(\theta) = \mathcal{L}_{cls}(\theta) + \lambda_2 \cdot \mathcal{L}_{fair}(\theta)$ 
11:     $\theta \leftarrow \theta - \eta_p \cdot \nabla_{\theta} \mathcal{L}(\theta)$ 
12:     $\lambda_2 \leftarrow \max\{\lambda_2 + \eta_d \cdot (\mathcal{L}_{fair}(\theta) - \gamma_2), 0\}$ 
13:  end for
14: until convergence
15: procedure DATAAUG( $\mathbf{x}, z, y$ )
16:    $\mathbf{c} = E^m(\mathbf{x}, \theta^m)$ 
17:   Sample  $\mathbf{s}' \sim \mathcal{N}(0, I_s)$ 
18:    $\mathbf{x}' = G^o(\mathbf{c}, \mathbf{s}', \phi_o)$ 
19:   return  $(\mathbf{x}', z, y)$ 
20: end procedure
```

Algorithm 4 FDDG w/o T (Ablation Study 2)

```
1: repeat
2:   for minibatch  $\mathcal{B} = \{(\mathbf{x}_i, z_i, y_i)\}_{i=1}^m \in \mathcal{D}_s$  do
3:      $\mathcal{L}_{cls}(\theta) = (1/m) \sum_{i=1}^m \ell(y_i, \hat{f}(\mathbf{x}_i, \theta))$ 
4:      $\mathcal{L}_{fair}(\theta) = (1/m) \sum_{i=1}^m (\frac{1}{p_1(1-p_1)} (\frac{z_i+1}{2} - p_1)) \hat{f}(\mathbf{x}_i, \theta)$ 
5:      $\mathcal{L}(\theta) = \mathcal{L}_{cls}(\theta) + \lambda_2 \cdot \mathcal{L}_{fair}(\theta)$ 
6:      $\theta \leftarrow \theta - \eta_p \cdot \nabla_{\theta} \mathcal{L}(\theta)$ 
7:      $\lambda_2 \leftarrow \max\{\lambda_2 + \eta_d \cdot (\mathcal{L}_{fair}(\theta) - \gamma_2), 0\}$ 
8:   end for
9: until convergence
```

where $e_i \in \mathcal{E}_s$. Taking average of upper bounds based on all source domains, we have:

$$\begin{aligned} \epsilon^{e_t}(f) &\leq \frac{1}{|\mathcal{E}_s|} \sum_{e_i \in \mathcal{E}_s} \epsilon^{e_i}(f) + \frac{\sqrt{2}}{|\mathcal{E}_s|} \sum_{e_i \in \mathcal{E}_s} D[\mathbb{P}(X^{e_t}, Z^{e_t}, Y^{e_t}), \mathbb{P}(X^{e_i}, Z^{e_i}, Y^{e_i})] \\ &\leq \frac{1}{|\mathcal{E}_s|} \sum_{e_i \in \mathcal{E}_s} \epsilon^{e_i}(f) + \frac{\sqrt{2}}{|\mathcal{E}_s|} |\mathcal{E}_s| D[\mathbb{P}(X^{e_t}, Z^{e_t}, Y^{e_t}), \mathbb{P}(X^{e_*}, Z^{e_*}, Y^{e_*})] \\ &\quad + \frac{\sqrt{2}}{|\mathcal{E}_s|} \sum_{e_i \in \mathcal{E}_s} D[\mathbb{P}(X^{e_*}, Z^{e_*}, Y^{e_*}), \mathbb{P}(X^{e_i}, Z^{e_i}, Y^{e_i})] \\ &\leq \frac{1}{|\mathcal{E}_s|} \sum_{e_i \in \mathcal{E}_s} \epsilon^{e_i}(f) + \sqrt{2} \min_{e_i \in \mathcal{E}_s} D[\mathbb{P}(X^{e_t}, Z^{e_t}, Y^{e_t}), \mathbb{P}(X^{e_i}, Z^{e_i}, Y^{e_i})] \\ &\quad + \sqrt{2} \max_{e_i, e_j \in \mathcal{E}_s} D[\mathbb{P}(X^{e_i}, Z^{e_i}, Y^{e_i}), \mathbb{P}(X^{e_j}, Z^{e_j}, Y^{e_j})] \end{aligned}$$

□

E.2 Sketch Proof of Theorem 2

Before we prove Theorem 2, we first make the following propositions and assumptions.

Algorithm 5 FDDG w/o fc (Ablation Study 3)

```

1: repeat
2:   for minibatch  $\mathcal{B} = \{(\mathbf{x}_i, z_i, y_i)\}_{i=1}^m \in \mathcal{D}_s$  do
3:      $\mathcal{L}_{cls}(\boldsymbol{\theta}) = (1/m) \sum_{i=1}^m \ell(y_i, \hat{f}(\mathbf{x}_i, \boldsymbol{\theta}))$ 
4:     Initialize  $\mathcal{L}'_{inv}(\boldsymbol{\theta}) = 0$ 
5:     for each  $(\mathbf{x}_i, z_i, y_i)$  in the minibatch do
6:        $(\mathbf{x}'_i, y_i) = \text{DATAAUG}(\mathbf{x}_i, z_i, y_i)$ 
7:        $\mathcal{L}'_{inv}(\boldsymbol{\theta}) += d[\hat{f}(\mathbf{x}_i, \boldsymbol{\theta}), \hat{f}(\mathbf{x}'_i, \boldsymbol{\theta})]$ 
8:     end for
9:      $\mathcal{L}_{inv}(\boldsymbol{\theta}) = \mathcal{L}'_{inv}(\boldsymbol{\theta})/m$ 
10:     $\mathcal{L}(\boldsymbol{\theta}) = \mathcal{L}_{cls}(\boldsymbol{\theta}) + \lambda_1 \cdot \mathcal{L}_{inv}(\boldsymbol{\theta})$ 
11:     $\boldsymbol{\theta} \leftarrow \boldsymbol{\theta} - \eta_p \cdot \nabla_{\boldsymbol{\theta}} \mathcal{L}(\boldsymbol{\theta})$ 
12:     $\lambda_1 \leftarrow \max\{\lambda_1 + \eta_d \cdot (\mathcal{L}_{inv}(\boldsymbol{\theta}) - \gamma_1), 0\}$ 
13:  end for
14: until convergence
15: procedure DATAAUG( $\mathbf{x}, z, y$ )
16:    $\mathbf{c} = E^c(E^m(\mathbf{x}, \boldsymbol{\theta}^m), \boldsymbol{\theta}^c)$ 
17:   Sample  $\mathbf{a}' \sim \mathcal{N}(0, I_a)$ 
18:   Sample  $\mathbf{s}' \sim \mathcal{N}(0, I_s)$ 
19:    $\mathbf{x}' = G^o(G^i(\mathbf{c}, \mathbf{a}', \phi_i), \mathbf{s}', \phi_o)$ 
20:   return  $(\mathbf{x}', z, y)$ 
21: end procedure

```

Proposition 1. Let d be a distance metric between probability measures for which it holds that $d[\mathbb{P}, \mathbb{T}] = 0$ for two distributions \mathbb{P} and \mathbb{T} if and only if $\mathbb{P} = \mathbb{T}$ almost surely. Then $P^*(0, 0) = P^*$

Proposition 2. Assuming the perturbation function $P^*(\gamma_1, \gamma_2)$ is L -lipschitz continuous in γ_1, γ_2 . Then given Proposition 1, it follows that $|P^* - P^*(\gamma_1, \gamma_2)| \leq L\|\gamma\|_1$, where $\gamma = [\gamma_1, \gamma_2]^T$.

Definition 4. Let $\Theta \subseteq \mathbb{R}^p$ be a finite-dimensional parameter space. For $\xi > 0$, a function $\hat{f} : \mathcal{X} \times \Theta \rightarrow \mathcal{Y}$ is said to be an ξ -parameterization of \mathcal{F} if it holds that for each $f \in \mathcal{F}$, there exists a parameter $\boldsymbol{\theta} \in \Theta$ such that $\mathbb{E}_{\mathbb{P}(\mathcal{X})} \|\hat{f}(\mathbf{x}, \boldsymbol{\theta}) - f(\mathbf{x})\|_{\infty} \leq \xi$. Given an ξ -parameterization \hat{f} of \mathcal{F} , consider the following saddle-point problem:

$$D_{\xi}^*(\gamma_1, \gamma_2) \triangleq \max_{\lambda_1(e_i, e_j), \lambda_2(e_i, e_j)} \min_{\boldsymbol{\theta} \in \Theta} R(\boldsymbol{\theta}) + \int_{e_i, e_j \in \mathcal{E}} [\delta^{e_i, e_j}(\boldsymbol{\theta}) - \gamma_1] d\lambda_1(e_i, e_j) \\ + \int_{e_i, e_j \in \mathcal{E}} [\epsilon^{e_i}(\boldsymbol{\theta}) + \epsilon^{e_j}(\boldsymbol{\theta}) - \gamma_2] d\lambda_2(e_i, e_j)$$

where $R(\boldsymbol{\theta}) = R(\hat{f}(\cdot, \boldsymbol{\theta}))$ and $\mathcal{L}^{e_i, e_j}(\boldsymbol{\theta}) = \mathcal{L}^{e_i, e_j}(\hat{f}(\cdot, \boldsymbol{\theta}))$.

Assumption 4. The loss function ℓ is non-negative, convex, and L_{ℓ} -Lipschitz continuous in its first argument,

$$|\ell(f_1(\mathbf{x}), y) - \ell(f_2(\mathbf{x}), y)| \leq \|f_1(\mathbf{x}) - f_2(\mathbf{x})\|_{\infty}$$

Assumption 5. The distance metric d is non-negative, convex, and satisfies the following uniform Lipschitz-like inequality for some constant $L_d > 0$:

$$|d[f_1(\mathbf{x}), f_1(\mathbf{x}' = T(\mathbf{x}, z, e))] - d[f_2(\mathbf{x}), f_2(\mathbf{x}' = T(\mathbf{x}, z, e))]| \leq L_d \|f_1(\mathbf{x}) - f_2(\mathbf{x})\|_{\infty}, \quad \forall e \in \mathcal{E}$$

Assumption 6. The fairness metric g is non-negative, convex, and satisfies the following uniform Lipschitz-like inequality for some constant $L_g > 0$:

$$|(g \circ f_1)(\mathbf{x}, z) - (g \circ f_2)(\mathbf{x}, z)| \leq L_g \|f_1(\mathbf{x}) - f_2(\mathbf{x})\|_{\infty}, \quad \forall e \in \mathcal{E}$$

Assumption 7. There exists a parameter $\boldsymbol{\theta} \in \Theta$ such that $\delta^{e_i, e_j}(\boldsymbol{\theta}) < \gamma_1 - \xi \cdot \max\{L_{\ell}, L_d\}$ and $\epsilon^{e_i}(\boldsymbol{\theta}) + \epsilon^{e_j}(\boldsymbol{\theta}) < \gamma_2 - \xi \cdot \max\{L_{\ell}, L_g\}, \forall e_i, e_j \in \mathcal{E}$

Proposition 3. Let $\gamma_1, \gamma_2 > 0$ be given. With the assumptions above, it holds that

$$P^*(\gamma_1, \gamma_2) \leq D_{\xi}^*(\gamma_1, \gamma_2) \leq P^*(\gamma_1, \gamma_2) + \xi(1 + \|\lambda_p^*\|_1) \cdot k$$

where λ_p^* is the optimal dual variable for a perturbed version of Eq. (5) in which the constraints are tightened to hold with margin $\gamma - \xi \cdot k$, $k = \max\{L_{\ell}, L_d, L_g\}$. In particular, this result implies that

$$|P^*(\gamma_1, \gamma_2) - D_{\xi}^*(\gamma_1, \gamma_2)| \leq \xi k(1 + \|\lambda_p^*\|_{L_1})$$

Table 6: Full performance on cCMNIST. (bold is the best; underline is the second best).

Methods	DP \uparrow / AUC \downarrow / Accuracy \uparrow			
	(R, 0.11)	(G, 0.43)	(B, 0.87)	Avg
RandAug	0.11 \pm 0.05 / 0.95 \pm 0.02 / 90.59 \pm 0.23	0.44 \pm 0.01 / 0.71 \pm 0.03 / 87.62 \pm 0.22	0.87 \pm 0.03 / 0.66 \pm 0.01 / 86.33 \pm 1.50	0.47 / 0.77 / 88.18
ERM	0.12 \pm 0.25 / 0.91 \pm 0.03 / 98.00 \pm 1.14	0.43 \pm 0.23 / 0.78 \pm 0.01 / 98.07 \pm 0.35	0.89 \pm 0.06 / 0.64 \pm 0.01 / 95.64 \pm 1.75	0.48 / 0.78 / 97.24
IRM	<u>0.21</u> \pm 0.15 / 0.97 \pm 0.02 / 75.50 \pm 2.11	0.28 \pm 0.10 / <u>0.64</u> \pm 0.01 / 92.74 \pm 0.27	0.76 \pm 0.12 / 0.63 \pm 0.03 / 80.05 \pm 2.34	0.42 / 0.75 / 82.76
GDRO	0.12 \pm 0.09 / 0.92 \pm 0.03 / 98.19 \pm 0.93	0.43 \pm 0.06 / 0.75 \pm 0.03 / 98.17 \pm 0.87	0.90 \pm 0.07 / 0.65 \pm 0.01 / 95.03 \pm 0.12	0.48 / 0.77 / 97.13
Mixup	0.12 \pm 0.21 / 0.92 \pm 0.02 / 97.89 \pm 1.97	0.41 \pm 0.06 / 0.79 \pm 0.02 / 98.00 \pm 1.36	0.93 \pm 0.04 / 0.65 \pm 0.01 / 96.09 \pm 1.07	0.49 / 0.79 / 97.32
MLDG	0.11 \pm 0.12 / 0.91 \pm 0.03 / <u>98.52</u> \pm 0.94	0.43 \pm 0.22 / 0.77 \pm 0.02 / 98.67 \pm 0.61	0.87 \pm 0.09 / 0.62 \pm 0.03 / 93.76 \pm 1.50	0.46 / 0.77 / 96.98
CORAL	0.11 \pm 0.08 / 0.91 \pm 0.03 / 98.69 \pm 0.76	0.42 \pm 0.20 / 0.79 \pm 0.02 / <u>98.30</u> \pm 0.98	0.87 \pm 0.07 / 0.64 \pm 0.01 / 93.74 \pm 1.54	0.47 / 0.78 / 96.91
MMD	0.11 \pm 0.08 / 0.92 \pm 0.01 / 98.69 \pm 1.07	0.41 \pm 0.21 / 0.73 \pm 0.03 / 97.72 \pm 1.31	0.93 \pm 0.04 / 0.59 \pm 0.01 / 95.37 \pm 1.56	0.48 / 0.75 / 97.26
DANN	0.14 \pm 0.08 / 0.87 \pm 0.03 / 85.94 \pm 1.76	0.17 \pm 0.13 / 0.90 \pm 0.03 / 84.93 \pm 0.67	0.76 \pm 0.17 / 0.63 \pm 0.03 / 84.04 \pm 1.75	0.36 / 0.80 / 84.97
CDANN	0.19 \pm 0.13 / 0.90 \pm 0.01 / 93.03 \pm 2.18	0.60 \pm 0.17 / 0.89 \pm 0.03 / 71.92 \pm 1.03	0.77 \pm 0.14 / 0.63 \pm 0.02 / 84.03 \pm 1.96	0.52 / 0.81 / 82.99
DDG	0.11 \pm 0.07 / 0.91 \pm 0.01 / 98.26 \pm 2.38	0.42 \pm 0.14 / 0.77 \pm 0.02 / 98.14 \pm 0.11	<u>0.96</u> \pm 0.03 / 0.60 \pm 0.01 / 97.02 \pm 1.70	0.50 / 0.76 / 97.81
MBDG	0.12 \pm 0.04 / 0.93 \pm 0.01 / 98.47 \pm 0.94	0.42 \pm 0.08 / 0.81 \pm 0.03 / 97.62 \pm 1.87	0.90 \pm 0.08 / 0.64 \pm 0.03 / 96.01 \pm 2.26	0.48 / 0.79 / <u>97.37</u>
DDG-FC	0.11 \pm 0.04 / 0.91 \pm 0.03 / 96.69 \pm 1.12	0.42 \pm 0.05 / 0.75 \pm 0.01 / 96.09 \pm 1.86	0.97 \pm 0.02 / <u>0.58</u> \pm 0.01 / 95.66 \pm 2.17	0.50 / 0.75 / 96.14
MBDG-FC	0.13 \pm 0.08 / 0.91 \pm 0.02 / 98.07 \pm 1.06	0.45 \pm 0.20 / 0.76 \pm 0.03 / 96.09 \pm 0.61	0.94 \pm 0.04 / 0.64 \pm 0.01 / 95.42 \pm 1.13	0.50 / 0.77 / 96.52
EIIL	0.15 \pm 0.08 / 0.94 \pm 0.03 / 81.00 \pm 0.31	0.26 \pm 0.06 / 0.98 \pm 0.01 / 82.67 \pm 2.44	0.62 \pm 0.16 / 0.98 \pm 0.01 / 71.68 \pm 0.51	0.34 / 0.97 / 78.45
FarconVAE	0.11 \pm 0.08 / 0.94 \pm 0.01 / 94.40 \pm 2.35	0.43 \pm 0.21 / 0.77 \pm 0.03 / 82.61 \pm 1.90	0.97 \pm 0.02 / 0.59 \pm 0.01 / 76.22 \pm 0.45	0.50 / 0.77 / 84.41
FATDM	0.17 \pm 0.03 / <u>0.86</u> \pm 0.02 / 96.00 \pm 0.23	<u>0.92</u> \pm 0.02 / <u>0.64</u> \pm 0.01 / 95.55 \pm 1.10	0.90 \pm 0.06 / 0.57 \pm 0.03 / 95.23 \pm 0.55	<u>0.66</u> / <u>0.67</u> / 95.59
FDDG	0.23 \pm 0.09 / 0.84 \pm 0.01 / 96.15 \pm 0.50	0.98 \pm 0.01 / 0.58 \pm 0.01 / 97.94 \pm 0.30	0.92 \pm 0.05 / 0.57 \pm 0.03 / <u>96.19</u> \pm 1.33	0.71 / 0.66 / 96.76

Proposition 4 (Empirical gap). Assume ℓ and d are non-negative and bounded in $[-B, B]$ and let d_{VC} denote the VC-dimension of the hypothesis class $\mathcal{A}_\xi = \{\hat{f}(\cdot, \theta) : \theta \in \Theta\} \subseteq \mathcal{F}$. Then it holds with probability $1 - \omega$ over the N samples from each domain that

$$|D_\xi^*(\gamma_1, \gamma_2) - D_{\xi, N, \mathcal{E}_s}^*(\gamma_1, \gamma_2)| \leq 2B \sqrt{\frac{1}{N} [1 + \log(\frac{4(2N)^{d_{VC}}}{\omega})]}$$

The Theorem 2. Let $\xi > 0$ be given, and let \hat{f} be an ξ -parameterization of \mathcal{F} . Let the assumptions holds, and further assume that ℓ , d , and g are $[0, B]$ -bounded and that $d[\mathbb{P}, \mathbb{T}] = 0$ if and only if $\mathbb{P} = \mathbb{T}$ almost surely, and that $P^*(\gamma_1, \gamma_2)$ is L -Lipschitz. Then assuming that $\mathcal{A}_\xi = \{\hat{f}(\cdot, \theta) : \theta \in \Theta\} \subseteq \mathcal{F}$ has finite VC-dimension, it holds with probability $1 - \omega$ over the N samples that

$$|P^* - D_{\xi, N, \mathcal{E}_s}^*(\gamma)| \leq L\|\gamma\|_1 + \xi k(1 + \|\lambda_p^*\|_1) + O(\sqrt{\log(M)/M})$$

Now we prove Theorem 2.

Proof. The proof of this theorem is a simple consequence of the triangle inequality. Indeed, by combining Proposition 2, Proposition 3, and Proposition 4, we find that

$$\begin{aligned} & |P^* - D_{\xi, N, \mathcal{E}_s}^*(\gamma_1, \gamma_2)| \\ &= |P^* + P^*(\gamma_1, \gamma_2) - P^*(\gamma_1, \gamma_2) + D_\xi^*(\gamma_1, \gamma_2) - D_\xi^*(\gamma_1, \gamma_2) - D_{\xi, N, \mathcal{E}_s}^*(\gamma_1, \gamma_2)| \\ &\leq |P^* - P^*(\gamma_1, \gamma_2)| + |P^*(\gamma_1, \gamma_2) - D_\xi^*(\gamma_1, \gamma_2)| + |D_\xi^*(\gamma_1, \gamma_2) - D_{\xi, N, \mathcal{E}_s}^*(\gamma_1, \gamma_2)| \\ &\leq L\|\gamma\|_1 + \xi k(1 + \|\lambda_p^*\|_1) + 2B \sqrt{\frac{1}{N} [1 + \log(\frac{4(2N)^{d_{VC}}}{\omega})]} \end{aligned}$$

□

F Additional Results

Additional results including more visualization (Fig. 6), as well as complete results with all domains and baselines on cCMNIST (Tab. 6), FairFace (Tab. 7), FairFace (Tab. 8), and NYSF (Tab. 9) are provided. Additional ablation study results are in Tabs. 10 to 13.

Trade-off between fairness-accuracy. In our algorithm, because λ_2 is the parameter that regularizes the fair loss, we conduct additional experiments to show the change between accuracy and fairness. Our results show that the larger (smaller) λ_2 , the better (worse) model fairness for each domain as well as in average, but it gives worse (better) model utility. Moreover, we show additional experiment results based on choosing different γ_1 and γ_2 . We observe that (1) by only increasing γ_2 , the model towards giving unfair outcomes but higher accuracy; (2) by only increasing γ_1 , performance on both model fairness and accuracy decreases. This may be due to the failure of disentanglement of factors. Evaluation on all datasets of fairness-accuracy trade-offs is given in Tab. 14. Results in the table are average performance over target domains.

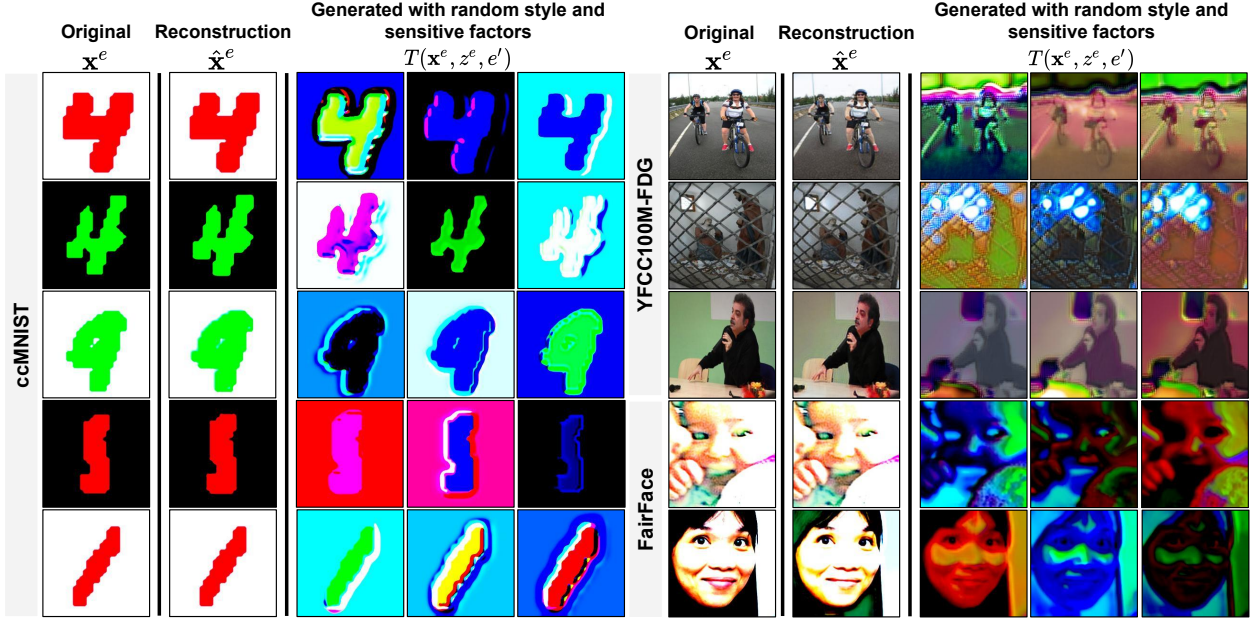


Figure 6: Additional visualizations for data reconstruction and under the transformation model T .

Table 7: Full performance on FairFace. (bold is the best; underline is the second best).

Methods	DP \uparrow / AUC \downarrow / Accuracy \uparrow		
	(B, 0.91)	(E, 0.87)	(I, 0.58)
RandAug	0.64 \pm 0.26 / 0.64 \pm 0.15 / 93.47 \pm 1.56	0.41 \pm 0.34 / 0.68 \pm 0.09 / 95.62 \pm 1.96	0.44 \pm 0.21 / 0.63 \pm 0.05 / 92.99 \pm 1.00
ERM	0.67 \pm 0.17 / 0.58 \pm 0.02 / 91.89 \pm 1.10	0.43 \pm 0.21 / 0.64 \pm 0.02 / <u>95.69\pm2.19</u>	0.50 \pm 0.19 / 0.59 \pm 0.03 / 93.28 \pm 1.61
IRM	0.63 \pm 0.12 / 0.58 \pm 0.01 / 93.39 \pm 1.03	0.32 \pm 0.23 / 0.63 \pm 0.03 / 95.12 \pm 0.49	0.45 \pm 0.06 / 0.59 \pm 0.02 / 92.01 \pm 1.13
GDRO	0.71 \pm 0.16 / 0.57 \pm 0.02 / 89.81 \pm 1.10	0.46 \pm 0.16 / 0.61 \pm 0.02 / 95.26 \pm 1.53	0.50 \pm 0.14 / 0.59 \pm 0.01 / 93.27 \pm 1.27
Mixup	0.58 \pm 0.19 / 0.59 \pm 0.02 / 92.46 \pm 0.69	0.40 \pm 0.04 / 0.61 \pm 0.02 / 93.31 \pm 1.42	0.42 \pm 0.09 / 0.59 \pm 0.02 / 93.42\pm2.43
MLDG	0.63 \pm 0.25 / 0.58 \pm 0.02 / 92.71 \pm 2.36	0.41 \pm 0.15 / 0.62 \pm 0.03 / 95.59 \pm 0.87	0.51 \pm 0.15 / 0.60 \pm 0.02 / 93.35 \pm 1.87
CORAL	0.69 \pm 0.19 / 0.58 \pm 0.01 / 92.09 \pm 2.03	0.34 \pm 0.24 / 0.64 \pm 0.01 / 95.91\pm1.44	<u>0.53\pm0.05</u> / 0.59 \pm 0.02 / 93.35 \pm 0.26
MMD	0.69 \pm 0.25 / 0.56 \pm 0.01 / 93.87 \pm 0.14	0.45 \pm 0.22 / 0.57\pm0.02 / 94.68 \pm 0.20	0.27 \pm 0.18 / 0.57\pm0.03 / 89.88 \pm 0.22
DANN	0.46 \pm 0.07 / 0.61 \pm 0.02 / 91.80 \pm 0.64	0.53 \pm 0.18 / 0.85 \pm 0.03 / 91.54 \pm 2.24	0.38 \pm 0.18 / 0.63 \pm 0.01 / 90.09 \pm 0.60
CDANN	0.62 \pm 0.24 / 0.59 \pm 0.03 / 91.22 \pm 0.33	0.43 \pm 0.10 / 0.66 \pm 0.02 / 94.75 \pm 2.23	0.43 \pm 0.18 / 0.61 \pm 0.01 / 92.41 \pm 1.68
DDG	0.60 \pm 0.20 / 0.59 \pm 0.02 / 91.76 \pm 1.03	0.36 \pm 0.15 / 0.63 \pm 0.02 / 95.52 \pm 2.35	0.49 \pm 0.17 / 0.59 \pm 0.01 / 92.35 \pm 2.04
MBDG	0.60 \pm 0.15 / 0.58 \pm 0.01 / 91.29 \pm 1.41	0.46 \pm 0.19 / 0.63 \pm 0.01 / 95.01 \pm 1.39	0.52 \pm 0.14 / <u>0.58\pm0.02</u> / 92.77 \pm 2.07
DDG-FC	0.61 \pm 0.06 / 0.58 \pm 0.03 / 92.27 \pm 1.65	0.39 \pm 0.18 / 0.64 \pm 0.03 / 95.51 \pm 2.36	0.45 \pm 0.17 / 0.58 \pm 0.03 / 93.38 \pm 0.52
MBDG-FC	0.70 \pm 0.15 / 0.56 \pm 0.03 / 92.12 \pm 0.43	0.35 \pm 0.07 / <u>0.60\pm0.01</u> / 95.54 \pm 1.80	0.56\pm0.07 / 0.57\pm0.01 / 92.41 \pm 1.61
EIIL	0.88 \pm 0.07 / 0.59 \pm 0.05 / 84.75 \pm 2.16	0.69 \pm 0.12 / 0.71 \pm 0.01 / 92.86 \pm 1.70	0.47 \pm 0.08 / 0.57\pm0.01 / 86.93 \pm 0.89
FarconVAE	<u>0.93\pm0.03</u> / 0.54\pm0.01 / 89.61 \pm 0.64	0.72 \pm 0.17 / 0.63 \pm 0.01 / 91.50 \pm 1.89	0.42 \pm 0.24 / <u>0.58\pm0.03</u> / 87.42 \pm 2.14
FATDM	<u>0.93\pm0.03</u> / 0.57 \pm 0.02 / 92.20 \pm 0.36	<u>0.80\pm0.02</u> / 0.65 \pm 0.02 / 92.89 \pm 1.00	0.52 \pm 0.10 / 0.60 \pm 0.01 / 92.22 \pm 1.60
FDDG	0.94\pm0.05 / <u>0.55\pm0.02</u> / 93.91\pm0.33	0.87\pm0.05 / <u>0.60\pm0.01</u> / 95.91\pm1.06	0.48 \pm 0.06 / 0.57\pm0.02 / 92.55 \pm 1.45

G Limitations

In Sec. 5 and Appendix F, we empirically demonstrate the effectiveness of the proposed FDDG, wherein our method is developed based on assumptions. We assume (1) data instances can be encoded into three latent factors, (2) such factors are independent of each other, and (3) each domain shares the same content space. FDDG may not work well when data are generated with more than three factors, and each is correlated to the other. To address such limitations, studies on causal learning could be a solution. Moreover, our model relies on domain augmentation. While the results demonstrate its effectiveness, it might not perform optimally when content spaces do not completely overlap across domains. In such scenarios, a preferable approach would involve initially augmenting data by minimizing semantic gaps for each class across training domains, followed by conducting domain augmentations.

Methods	DP \uparrow / AUC \downarrow / Accuracy \uparrow		
	(M, 0.87)	(S, 0.39)	(W, 0.49)
RandAug	0.36 \pm 0.12 / 0.65 \pm 0.05 / 92.79 \pm 1.22	0.35 \pm 0.20 / 0.69 \pm 0.06 / 91.89 \pm 1.02	0.34 \pm 0.09 / 0.64 \pm 0.02 / 92.07 \pm 0.55
ERM	0.34 \pm 0.08 / 0.62 \pm 0.01 / 92.51 \pm 1.45	0.68 \pm 0.14 / 0.59 \pm 0.03 / 93.48 \pm 0.94	0.39 \pm 0.09 / 0.61 \pm 0.01 / 92.82 \pm 0.38
IRM	0.34 \pm 0.11 / 0.65 \pm 0.02 / 92.47 \pm 2.42	0.55 \pm 0.23 / 0.59 \pm 0.01 / 91.81 \pm 0.66	0.32 \pm 0.19 / 0.66 \pm 0.01 / 90.54 \pm 1.56
GDRO	0.45 \pm 0.14 / 0.63 \pm 0.02 / 91.75 \pm 1.11	0.72 \pm 0.14 / 0.59 \pm 0.01 / 93.65 \pm 0.67	0.48 \pm 0.09 / 0.60 \pm 0.01 / 92.50 \pm 0.38
Mixup	0.31 \pm 0.11 / 0.62 \pm 0.02 / 93.52 \pm 0.79	0.91 \pm 0.04 / 0.58 \pm 0.02 / 93.20 \pm 0.33	0.43 \pm 0.19 / 0.61 \pm 0.01 / <u>92.98</u> \pm 0.03
MLDG	0.35 \pm 0.20 / 0.62 \pm 0.01 / 92.45 \pm 0.07	0.71 \pm 0.22 / 0.57 \pm 0.01 / 93.85 \pm 0.40	0.47 \pm 0.20 / 0.59 \pm 0.01 / 92.82 \pm 1.65
CORAL	0.43 \pm 0.08 / 0.63 \pm 0.01 / 92.23 \pm 0.06	0.74 \pm 0.10 / 0.58 \pm 0.01 / 93.77 \pm 1.99	0.50 \pm 0.14 / 0.60 \pm 0.02 / 92.47 \pm 2.04
MMD	0.48 \pm 0.25 / 0.62 \pm 0.02 / 91.07 \pm 2.00	0.66 \pm 0.18 / 0.59 \pm 0.03 / 92.58 \pm 1.63	0.39 \pm 0.20 / 0.68 \pm 0.02 / 91.75 \pm 1.37
DANN	0.65 \pm 0.14 / 0.88 \pm 0.01 / 91.46 \pm 0.50	0.80 \pm 0.14 / 0.57 \pm 0.02 / 88.20 \pm 1.65	0.11 \pm 0.09 / 0.66 \pm 0.01 / 86.80 \pm 1.18
CDANN	0.27 \pm 0.12 / 0.67 \pm 0.01 / 91.07 \pm 0.97	0.52 \pm 0.12 / 0.82 \pm 0.02 / 88.32 \pm 0.37	0.35 \pm 0.17 / 0.67 \pm 0.02 / 90.19 \pm 0.60
DDG	0.37 \pm 0.14 / 0.64 \pm 0.01 / 91.36 \pm 0.65	0.63 \pm 0.22 / 0.58 \pm 0.01 / 93.40 \pm 0.37	<u>0.51</u> \pm 0.07 / 0.60 \pm 0.01 / 91.34 \pm 0.80
MBDG	0.38 \pm 0.14 / 0.64 \pm 0.02 / 92.23 \pm 1.15	0.67 \pm 0.06 / <u>0.56</u> \pm 0.03 / 93.12 \pm 0.70	0.30 \pm 0.04 / 0.62 \pm 0.01 / 91.05 \pm 0.53
DDG-FC	0.42 \pm 0.09 / 0.95 \pm 0.03 / 92.70 \pm 1.49	0.76 \pm 0.21 / 0.59 \pm 0.02 / 93.85 \pm 1.79	0.48 \pm 0.15 / 0.62 \pm 0.02 / 92.45 \pm 1.55
MBDG-FC	0.49 \pm 0.19 / 0.63 \pm 0.03 / 90.67 \pm 0.42	0.74 \pm 0.23 / 0.57 \pm 0.01 / 93.24 \pm 0.32	0.32 \pm 0.07 / 0.60 \pm 0.03 / 91.50 \pm 0.57
EIIL	0.52 \pm 0.09 / 0.63 \pm 0.03 / 84.96 \pm 1.37	0.98 \pm 0.01 / 0.55 \pm 0.02 / 89.99 \pm 2.27	0.46 \pm 0.05 / 0.65 \pm 0.03 / 86.53 \pm 1.02
FarconVAE	0.54 \pm 0.22 / 0.58 \pm 0.02 / 85.62 \pm 1.49	<u>0.92</u> \pm 0.06 / <u>0.56</u> \pm 0.10 / 90.00 \pm 0.05	<u>0.51</u> \pm 0.07 / 0.60 \pm 0.01 / 86.40 \pm 0.42
FATDM	<u>0.55</u> \pm 0.12 / 0.65 \pm 0.01 / 92.23 \pm 1.56	<u>0.92</u> \pm 0.10 / 0.57 \pm 0.02 / 92.36 \pm 0.99	0.46 \pm 0.05 / 0.63 \pm 0.01 / 92.56 \pm 0.31
FDDG	0.54 \pm 0.08 / <u>0.62</u> \pm 0.02 / 92.61 \pm 1.84	0.98 \pm 0.01 / 0.55 \pm 0.01 / 92.26 \pm 2.48	0.52 \pm 0.17 / 0.58 \pm 0.03 / 93.02 \pm 0.50

Methods	DP \uparrow / AUC \downarrow / Accuracy \uparrow	
	(L, 0.48)	Avg
RandAug	0.39 \pm 0.10 / 0.70 \pm 0.02 / 91.77 \pm 0.61	0.42 / 0.66 / 92.94
ERM	0.57 \pm 0.15 / 0.62 \pm 0.01 / 91.96 \pm 0.51	0.51 / 0.61 / 93.08
IRM	0.41 \pm 0.021 / 0.63 \pm 0.05 / 92.06 \pm 1.89	0.43 / 0.62 / 92.48
GDRO	0.54 \pm 0.15 / 0.62 \pm 0.01 / 91.59 \pm 0.51	0.55 / <u>0.60</u> / 92.55
Mixup	0.55 \pm 0.22 / 0.61 \pm 0.02 / 93.43 \pm 2.02	0.51 / <u>0.60</u> / 93.19
MLDG	0.53 \pm 0.18 / 0.62 \pm 0.03 / 92.99 \pm 0.86	0.51 / <u>0.60</u> / 93.39
CORAL	0.56 \pm 0.23 / 0.59 \pm 0.03 / 92.62 \pm 1.11	0.54 / <u>0.60</u> / 93.21
MMD	0.55 \pm 0.16 / 0.61 \pm 0.02 / 92.53 \pm 1.41	0.50 / <u>0.60</u> / 92.34
DANN	0.39 \pm 0.21 / 0.67 \pm 0.01 / 90.82 \pm 2.44	0.47 / 0.70 / 90.10
CDANN	0.42 \pm 0.23 / 0.61 \pm 0.03 / 92.42 \pm 2.19	0.43 / 0.66 / 91.48
DDG	0.44 \pm 0.17 / 0.62 \pm 0.02 / 93.46 \pm 0.32	0.49 / 0.61 / 92.74
MBDG	0.56 \pm 0.09 / 0.61 \pm 0.01 / <u>93.49</u> \pm 0.97	0.50 / <u>0.60</u> / 92.71
DDG-FC	0.50 \pm 0.25 / 0.62 \pm 0.03 / 92.42 \pm 0.30	0.52 / 0.61 / 93.23
MBDG-FC	<u>0.57</u> \pm 0.23 / 0.62 \pm 0.02 / 91.89 \pm 0.81	0.53 / <u>0.60</u> / 92.48
EIIL	0.49 \pm 0.07 / 0.59 \pm 0.01 / 88.39 \pm 1.25	0.64 / 0.61 / 87.78
FarconVAE	0.58 \pm 0.05 / <u>0.60</u> \pm 0.05 / 88.70 \pm 0.71	0.66 / 0.58 / 88.46
FATDM	0.51 \pm 0.16 / 0.63 \pm 0.02 / 93.33 \pm 0.20	<u>0.67</u> / 0.61 / 92.54
FDDG	0.58 \pm 0.15 / 0.59 \pm 0.01 / 93.73 \pm 0.26	0.70 / 0.58 / 93.42

Table 8: Full performance on YFCC100M-FDG. (bold is the best; underline is the second best).

Methods	DP \uparrow / AUC \downarrow / Accuracy \uparrow			
	(d_0 , 0.73)	(d_1 , 0.84)	(d_2 , 0.72)	Avg
RandAug	0.67 \pm 0.06 / 0.57 \pm 0.02 / 57.47 \pm 1.20	0.67 \pm 0.34 / 0.61 \pm 0.01 / 82.43 \pm 1.25	0.65 \pm 0.21 / 0.64 \pm 0.02 / 87.88 \pm 0.35	0.66 / 0.61 / 75.93
ERM	0.81 \pm 0.09 / 0.58 \pm 0.01 / 40.51 \pm 0.23	0.71 \pm 0.18 / 0.66 \pm 0.03 / 83.91 \pm 0.33	0.89 \pm 0.08 / 0.59 \pm 0.01 / 82.06 \pm 0.33	0.80 / 0.61 / 68.83
IRM	0.76 \pm 0.10 / 0.58 \pm 0.02 / 50.51 \pm 2.44	0.87 \pm 0.08 / 0.60 \pm 0.02 / 73.26 \pm 0.03	0.70 \pm 0.24 / 0.57 \pm 0.02 / 82.78 \pm 2.19	0.78 / 0.58 / 68.85
GDRO	0.80 \pm 0.05 / 0.59 \pm 0.01 / 53.43 \pm 2.29	0.73 \pm 0.22 / 0.60 \pm 0.01 / 87.56 \pm 2.20	0.79 \pm 0.13 / 0.65 \pm 0.02 / 83.10 \pm 0.64	0.78 / 0.62 / 74.70
Mixup	0.82 \pm 0.07 / 0.57 \pm 0.03 / 61.15 \pm 0.28	0.79 \pm 0.14 / 0.63 \pm 0.03 / 78.63 \pm 0.97	0.89 \pm 0.05 / 0.60 \pm 0.01 / 85.18 \pm 0.80	0.84 / 0.60 / 74.99
MLDG	0.75 \pm 0.13 / 0.67 \pm 0.01 / 49.56 \pm 0.69	0.71 \pm 0.19 / 0.57 \pm 0.02 / 89.45 \pm 0.44	0.71 \pm 0.14 / 0.57 \pm 0.03 / 87.51 \pm 0.18	0.72 / 0.60 / 75.51
CORAL	0.80 \pm 0.11 / 0.58 \pm 0.02 / 58.96 \pm 2.34	0.72 \pm 0.11 / 0.64 \pm 0.03 / 91.66 \pm 0.85	0.70 \pm 0.07 / 0.64 \pm 0.03 / 89.28 \pm 1.77	0.74 / 0.62 / 79.97
MMD	0.79 \pm 0.11 / 0.59 \pm 0.02 / 61.51 \pm 1.79	0.71 \pm 0.15 / 0.64 \pm 0.03 / 91.15 \pm 2.33	0.79 \pm 0.17 / 0.60 \pm 0.01 / 86.69 \pm 0.19	0.76 / 0.61 / 79.87
DANN	0.70 \pm 0.13 / 0.78 \pm 0.02 / 47.71 \pm 1.56	0.79 \pm 0.12 / <u>0.53</u> \pm 0.01 / 84.80 \pm 1.14	0.77 \pm 0.17 / 0.59 \pm 0.02 / 58.50 \pm 1.74	0.75 / 0.64 / 63.67
CDANN	0.74 \pm 0.13 / 0.58 \pm 0.02 / 55.87 \pm 2.09	0.70 \pm 0.22 / 0.65 \pm 0.02 / 87.06 \pm 2.43	0.72 \pm 0.13 / 0.63 \pm 0.02 / 85.76 \pm 2.43	0.72 / 0.62 / 76.23
DDG	0.81 \pm 0.14 / 0.57 \pm 0.03 / 60.08 \pm 1.08	0.74 \pm 0.12 / 0.66 \pm 0.03 / 92.53 \pm 0.91	0.71 \pm 0.21 / 0.59 \pm 0.03 / 95.02 \pm 1.92	0.75 / 0.61 / 82.54
MBDG	0.79 \pm 0.15 / 0.58 \pm 0.01 / 60.46 \pm 1.90	0.73 \pm 0.07 / 0.67 \pm 0.01 / 94.36 \pm 0.23	0.71 \pm 0.11 / 0.59 \pm 0.03 / <u>93.48</u> \pm 0.65	0.74 / 0.61 / <u>82.77</u>
DDG-FC	0.76 \pm 0.06 / 0.58 \pm 0.03 / 59.96 \pm 2.36	0.83 \pm 0.06 / 0.58 \pm 0.01 / 96.80 \pm 1.28	0.82 \pm 0.09 / 0.59 \pm 0.01 / 86.38 \pm 2.45	0.80 / 0.58 / 81.04
MBDG-FC	0.80 \pm 0.13 / 0.58 \pm 0.01 / <u>62.31</u> \pm 0.13	0.72 \pm 0.09 / 0.63 \pm 0.01 / <u>94.73</u> \pm 2.09	0.80 \pm 0.07 / 0.53 \pm 0.01 / 87.78 \pm 2.11	0.77 / 0.58 / 81.61
EIIL	0.87 \pm 0.11 / <u>0.55</u> \pm 0.02 / 56.74 \pm 0.60	0.76 \pm 0.05 / 0.54 \pm 0.03 / 68.99 \pm 0.91	0.87 \pm 0.06 / 0.78 \pm 0.03 / 72.19 \pm 0.75	0.83 / 0.62 / 65.98
FarconVAE	0.67 \pm 0.06 / 0.61 \pm 0.03 / 51.21 \pm 0.61	<u>0.90</u> \pm 0.06 / 0.59 \pm 0.01 / 72.40 \pm 2.13	0.85 \pm 0.12 / <u>0.55</u> \pm 0.01 / 74.20 \pm 2.46	0.81 / 0.58 / 65.93
FATDM	0.80 \pm 0.10 / <u>0.55</u> \pm 0.01 / 61.56 \pm 0.89	0.88 \pm 0.08 / 0.56 \pm 0.01 / 90.00 \pm 0.66	0.86 \pm 0.10 / 0.60 \pm 0.02 / 89.12 \pm 1.30	<u>0.84</u> / <u>0.57</u> / 80.22
FDDG	0.87 \pm 0.09 / 0.53 \pm 0.01 / 62.56 \pm 2.25	0.94 \pm 0.05 / 0.52 \pm 0.01 / 93.36 \pm 1.70	0.93 \pm 0.03 / 0.53 \pm 0.02 / 93.43 \pm 0.73	0.92 / 0.53 / 83.12

Table 9: Full performance on NYSE. (bold is the best; underline is the second best).

Methods	DP \uparrow / AUC \downarrow / Accuracy \uparrow		
	(R, 0.93)	(B, 0.85)	(M, 0.81)
ERM	0.91 \pm 0.07 / 0.53 \pm 0.01 / 60.21 \pm 1.48	0.90 \pm 0.07 / 0.54 \pm 0.01 / 58.93 \pm 1.10	0.92 \pm 0.04 / 0.54 \pm 0.01 / 59.49 \pm 1.50
IRM	0.98 \pm 0.01 / 0.52 \pm 0.02 / 61.61 \pm 0.80	0.94 \pm 0.04 / 0.52 \pm 0.02 / 56.89 \pm 0.73	0.92 \pm 0.02 / 0.53 \pm 0.03 / 59.64 \pm 2.33
GDRO	0.81 \pm 0.18 / 0.56 \pm 0.02 / 58.73 \pm 2.23	0.89 \pm 0.07 / 0.55 \pm 0.03 / 59.44 \pm 1.66	0.87 \pm 0.08 / 0.55 \pm 0.02 / 62.57 \pm 0.91
Mixup	0.96 \pm 0.03 / 0.53 \pm 0.01 / 62.63 \pm 1.84	0.90 \pm 0.06 / 0.54 \pm 0.04 / 58.96 \pm 2.89	0.92 \pm 0.04 / 0.54 \pm 0.03 / 58.29 \pm 0.80
MLDG	0.96 \pm 0.03 / 0.52 \pm 0.02 / 61.81 \pm 0.53	0.90 \pm 0.08 / 0.55 \pm 0.01 / 58.11 \pm 0.13	0.93 \pm 0.02 / 0.53 \pm 0.02 / 58.27 \pm 0.47
CORAL	0.95 \pm 0.02 / 0.52 \pm 0.02 / 62.17 \pm 0.92	0.93 \pm 0.04 / 0.54 \pm 0.01 / 58.06 \pm 1.99	0.95 \pm 0.03 / 0.53 \pm 0.01 / 58.84 \pm 0.74
MMD	0.91 \pm 0.05 / 0.53 \pm 0.01 / 60.34 \pm 1.39	0.89 \pm 0.07 / 0.55 \pm 0.02 / 58.47 \pm 0.35	0.92 \pm 0.02 / 0.54 \pm 0.01 / 59.31 \pm 0.40
DANN	0.83 \pm 0.13 / 0.52 \pm 0.02 / 40.80 \pm 2.47	0.96 \pm 0.02 / 0.55 \pm 0.03 / 54.55 \pm 0.17	0.88 \pm 0.04 / 0.52 \pm 0.01 / 59.19 \pm 1.21
CDANN	0.95 \pm 0.03 / 0.52 \pm 0.01 / 57.61 \pm 0.68	0.94 \pm 0.03 / 0.54 \pm 0.02 / 56.97 \pm 1.29	0.87 \pm 0.09 / 0.52 \pm 0.02 / 59.59 \pm 1.74
DDG	0.92 \pm 0.03 / 0.52 \pm 0.01 / 56.52 \pm 0.71	0.92 \pm 0.04 / 0.54 \pm 0.04 / 58.21 \pm 1.40	0.92 \pm 0.07 / 0.53 \pm 0.02 / 60.91 \pm 2.47
MBDG	0.96 \pm 0.02 / 0.52 \pm 0.01 / 55.96 \pm 1.37	0.90 \pm 0.07 / 0.70 \pm 0.01 / 51.52 \pm 1.55	0.96 \pm 0.02 / 0.53 \pm 0.03 / 58.74 \pm 2.46
DDG-FC	0.95 \pm 0.03 / 0.52 \pm 0.01 / 54.53 \pm 1.44	0.93 \pm 0.02 / 0.53 \pm 0.03 / 59.32 \pm 0.59	0.92 \pm 0.04 / 0.52 \pm 0.01 / 60.08 \pm 1.31
MBDG-FC	0.96 \pm 0.02 / 0.55 \pm 0.02 / 55.93 \pm 1.98	0.91 \pm 0.07 / 0.54 \pm 0.03 / 55.50 \pm 0.55	0.90 \pm 0.06 / 0.53 \pm 0.02 / 57.37 \pm 2.39
EIIL	0.95 \pm 0.02 / 0.52 \pm 0.02 / 58.28 \pm 3.23	0.92 \pm 0.03 / 0.54 \pm 0.02 / 56.76 \pm 3.87	0.83 \pm 0.11 / 0.54 \pm 0.02 / 59.47 \pm 1.69
FarconVAE	0.90 \pm 0.07 / 0.53 \pm 0.03 / 60.52 \pm 0.14	0.89 \pm 0.05 / 0.55 \pm 0.04 / 60.30 \pm 0.64	0.82 \pm 0.07 / 0.56 \pm 0.01 / 60.31 \pm 0.40
FATDM	0.93 \pm 0.05 / 0.52 \pm 0.01 / 59.32 \pm 1.00	0.86 \pm 0.05 / 0.58 \pm 0.02 / 59.01 \pm 0.32	0.85 \pm 0.08 / 0.53 \pm 0.02 / 60.45 \pm 0.87
FDDG	0.99 \pm 0.00 / 0.50 \pm 0.00 / 62.01 \pm 1.87	0.96 \pm 0.01 / 0.52 \pm 0.02 / 58.37 \pm 0.67	0.92 \pm 0.02 / 0.52 \pm 0.02 / 59.49 \pm 1.93

Methods	DP \uparrow / AUC \downarrow / Accuracy \uparrow		
	(Q, 0.59)	(S, 0.62)	Avg
ERM	0.88 \pm 0.06 / 0.57 \pm 0.02 / 62.48 \pm 0.64	0.86 \pm 0.12 / 0.61 \pm 0.03 / 54.54 \pm 0.68	0.90 / 0.56 / 59.13
IRM	0.87 \pm 0.06 / 0.54 \pm 0.01 / 55.81 \pm 1.74	0.89 \pm 0.07 / 0.54 \pm 0.03 / 57.00 \pm 2.01	0.92 / 0.53 / 58.19
GDRO	0.86 \pm 0.05 / 0.57 \pm 0.01 / 62.92 \pm 1.17	0.77 \pm 0.08 / 0.64 \pm 0.04 / 60.44 \pm 2.86	0.84 / 0.57 / 60.82
Mixup	0.93 \pm 0.04 / 0.53 \pm 0.01 / 61.34 \pm 1.60	0.84 \pm 0.08 / 0.61 \pm 0.02 / 53.07 \pm 3.13	0.91 / 0.55 / 58.86
MLDG	0.89 \pm 0.08 / 0.56 \pm 0.02 / 62.85 \pm 2.38	0.85 \pm 0.05 / 0.59 \pm 0.03 / 54.42 \pm 0.02	0.91 / 0.55 / 59.10
CORAL	0.95 \pm 0.03 / 0.53 \pm 0.02 / 61.45 \pm 0.28	0.88 \pm 0.08 / 0.54 \pm 0.03 / 52.08 \pm 1.06	0.93 / 0.53 / 58.52
MMD	0.88 \pm 0.03 / 0.56 \pm 0.01 / 62.48 \pm 1.31	0.81 \pm 0.17 / 0.61 \pm 0.02 / 57.73 \pm 1.54	0.88 / 0.56 / 59.67
DANN	0.96 \pm 0.02 / 0.53 \pm 0.02 / 63.60 \pm 0.34	0.86 \pm 0.05 / 0.56 \pm 0.03 / 58.96 \pm 0.98	0.90 / 0.54 / 55.42
CDANN	0.97 \pm 0.02 / 0.54 \pm 0.03 / 64.25 \pm 1.25	0.74 \pm 0.16 / 0.60 \pm 0.01 / 57.73 \pm 1.89	0.89 / 0.54 / 59.23
DDG	0.89 \pm 0.07 / 0.55 \pm 0.01 / 56.68 \pm 0.87	0.84 \pm 0.07 / 0.58 \pm 0.03 / 54.91 \pm 1.33	0.90 / 0.54 / 57.44
MBDG	0.96 \pm 0.03 / 0.52 \pm 0.01 / 60.73 \pm 1.56	0.90 \pm 0.04 / 0.52 \pm 0.02 / 52.45 \pm 1.98	0.93 / 0.56 / 55.88
DDG-FC	0.92 \pm 0.02 / 0.54 \pm 0.02 / 59.90 \pm 1.75	0.90 \pm 0.05 / 0.57 \pm 0.02 / 57.45 \pm 0.08	0.92 / 0.53 / 58.26
MBDG-FC	0.94 \pm 0.04 / 0.52 \pm 0.01 / 61.04 \pm 2.31	0.91 \pm 0.06 / 0.53 \pm 0.03 / 52.57 \pm 0.92	0.92 / 0.53 / 56.48
EIIL	0.84 \pm 0.12 / 0.55 \pm 0.02 / 52.18 \pm 0.26	0.95 \pm 0.03 / 0.59 \pm 0.02 / 55.74 \pm 0.12	0.90 / 0.54 / 56.49
FarconVAE	0.97 \pm 0.02 / 0.56 \pm 0.03 / 61.30 \pm 1.14	0.86 \pm 0.10 / 0.58 \pm 0.02 / 60.70 \pm 1.48	0.89 / 0.56 / 60.62
FATDM	0.85 \pm 0.05 / 0.52 \pm 0.01 / 60.35 \pm 0.44	0.88 \pm 0.03 / 0.52 \pm 0.01 / 59.22 \pm 0.09	0.87 / 0.53 / 59.67
FDDG	0.99 \pm 0.01 / 0.50 \pm 0.00 / 59.11 \pm 0.94	0.98 \pm 0.02 / 0.53 \pm 0.01 / 60.77 \pm 0.23	0.97 / 0.51 / 59.95

Table 10: Ablation studies results on cCMNIST.

Methods	DP \uparrow / AUC \downarrow / Accuracy \uparrow			
	(R, 0.11)	(G, 0.43)	(B, 0.87)	Avg
FDDG w/o sf	0.23 \pm 0.05 / 0.98 \pm 0.01 / 94.89 \pm 1.72	0.11 \pm 0.06 / 0.92 \pm 0.02 / 98.19 \pm 1.39	0.42 \pm 0.06 / 0.72 \pm 0.03 / 95.28 \pm 0.22	0.25 / 0.87 / 96.12
FDDG w/o T	0.21 \pm 0.12 / 0.92 \pm 0.01 / 96.74 \pm 1.15	0.15 \pm 0.08 / 0.86 \pm 0.02 / 96.95 \pm 0.93	0.48 \pm 0.06 / 0.57 \pm 0.02 / 96.05 \pm 1.17	0.28 / 0.79 / 96.58
FDDG w/o fc	0.22 \pm 0.08 / 0.91 \pm 0.02 / 96.63 \pm 0.63	0.44 \pm 0.16 / 0.75 \pm 0.01 / 97.90 \pm 0.40	0.97 \pm 0.02 / 0.61 \pm 0.02 / 96.01 \pm 0.20	0.54 / 0.76 / 96.85

Table 11: Ablation studies results on FairFace.

Methods	DP \uparrow / AUC \downarrow / Accuracy \uparrow		
	(B, 0.91)	(E, 0.87)	(I, 0.58)
FDDG w/o sf	0.68 \pm 0.18 / 0.57 \pm 0.02 / 93.07 \pm 0.68	0.43 \pm 0.20 / 0.60 \pm 0.03 / 95.55 \pm 2.09	0.37 \pm 0.09 / 0.59 \pm 0.03 / 92.26 \pm 0.37
FDDG w/o T	0.83 \pm 0.08 / 0.56 \pm 0.01 / 92.81 \pm 0.81	0.50 \pm 0.22 / 0.56 \pm 0.01 / 95.12 \pm 0.73	0.42 \pm 0.17 / 0.59 \pm 0.02 / 92.34 \pm 0.14
FDDG w/o fc	0.59 \pm 0.16 / 0.58 \pm 0.01 / 92.92 \pm 1.35	0.36 \pm 0.08 / 0.62 \pm 0.03 / 95.55 \pm 1.84	0.42 \pm 0.20 / 0.62 \pm 0.02 / 93.35 \pm 0.83

Methods	DP \uparrow / AUC \downarrow / Accuracy \uparrow		
	(M, 0.87)	(S, 0.39)	(W, 0.49)
FDDG w/o sf	0.49 \pm 0.13 / 0.62 \pm 0.03 / 92.61 \pm 2.32	0.69 \pm 0.22 / 0.56 \pm 0.01 / 93.28 \pm 2.31	0.35 \pm 0.26 / 0.58 \pm 0.01 / 92.18 \pm 0.46
FDDG w/o T	0.39 \pm 0.07 / 0.68 \pm 0.01 / 91.46 \pm 2.05	0.92 \pm 0.06 / 0.56 \pm 0.01 / 87.87 \pm 1.25	0.52 \pm 0.23 / 0.59 \pm 0.01 / 90.78 \pm 0.31
FDDG w/o fc	0.38 \pm 0.15 / 0.72 \pm 0.03 / 92.27 \pm 0.02	0.42 \pm 0.16 / 0.67 \pm 0.03 / 92.17 \pm 0.99	0.34 \pm 0.08 / 0.72 \pm 0.03 / 91.88 \pm 0.67

Methods	DP \uparrow / AUC \downarrow / Accuracy \uparrow	
	(L, 0.48)	Avg
FDDG w/o sf	0.47 \pm 0.07 / 0.63 \pm 0.01 / 92.62 \pm 0.93	0.49 / 0.59 / 93.08
FDDG w/o T	0.53 \pm 0.03 / 0.59 \pm 0.01 / 91.19 \pm 0.57	0.58 / 0.59 / 91.65
FDDG w/o fc	0.40 \pm 0.07 / 0.70 \pm 0.02 / 92.96 \pm 0.85	0.42 / 0.66 / 93.01

Table 12: Ablation studies results on YFCC100M-FDG.

Methods	DP \uparrow / AUC \downarrow / Accuracy \uparrow			
	(d_0 , 0.73)	(d_1 , 0.84)	(d_2 , 0.72)	Avg
FDDG w/o sf	0.69 \pm 0.13 / 0.57 \pm 0.02 / 43.09 \pm 1.45	0.83 \pm 0.08 / 0.63 \pm 0.02 / 89.68 \pm 0.60	0.89 \pm 0.05 / 0.54 \pm 0.03 / 87.70 \pm 1.69	0.80 / 0.58 / 73.49
FDDG w/o T	0.82 \pm 0.12 / 0.56 \pm 0.03 / 47.21 \pm 1.17	0.83 \pm 0.05 / 0.63 \pm 0.01 / 73.10 \pm 0.26	0.82 \pm 0.08 / 0.53 \pm 0.02 / 72.95 \pm 2.25	0.82 / 0.57 / 64.42
FDDG w/o fc	0.72 \pm 0.17 / 0.69 \pm 0.03 / 54.24 \pm 1.75	0.92 \pm 0.02 / 0.64 \pm 0.03 / 94.35 \pm 2.35	0.92 \pm 0.07 / 0.64 \pm 0.03 / 93.20 \pm 2.17	0.86 / 0.66 / 80.59

Table 13: Ablation studies results on NYSF.

Methods	DP \uparrow / AUC \downarrow / Accuracy \uparrow		
	(R, 0.93)	(B, 0.85)	(M, 0.81)
FDDG w/o sf	0.95 \pm 0.02 / 0.52 \pm 0.01 / 55.78 \pm 1.01	0.97 \pm 0.01 / 0.51 \pm 0.01 / 55.30 \pm 1.08	0.95 \pm 0.03 / 0.53 \pm 0.01 / 58.29 \pm 0.80
FDDG w/o T	0.95 \pm 0.03 / 0.52 \pm 0.01 / 61.36 \pm 0.42	0.91 \pm 0.06 / 0.54 \pm 0.01 / 57.67 \pm 0.82	0.89 \pm 0.05 / 0.55 \pm 0.01 / 60.68 \pm 0.31
FDDG w/o fc	0.95 \pm 0.02 / 0.52 \pm 0.02 / 63.72 \pm 0.37	0.87 \pm 0.09 / 0.55 \pm 0.01 / 58.86 \pm 0.68	0.89 \pm 0.08 / 0.54 \pm 0.01 / 60.61 \pm 0.59

Methods	DP \uparrow / AUC \downarrow / Accuracy \uparrow		
	(Q, 0.59)	(S, 0.62)	Avg
FDDG w/o sf	0.92 \pm 0.06 / 0.54 \pm 0.02 / 57.61 \pm 1.30	0.90 \pm 0.02 / 0.59 \pm 0.02 / 52.82 \pm 1.20	0.94 / 0.53 / 55.96
FDDG w/o T	0.97 \pm 0.02 / 0.52 \pm 0.01 / 59.33 \pm 0.17	0.87 \pm 0.11 / 0.57 \pm 0.01 / 55.40 \pm 0.73	0.92 / 0.54 / 58.89
FDDG w/o fc	0.83 \pm 0.08 / 0.57 \pm 0.01 / 64.17 \pm 0.35	0.89 \pm 0.06 / 0.58 \pm 0.02 / 56.51 \pm 0.84	0.89 / 0.55 / 60.77

Table 14: Trade-off between fairness-accuracy.

	DP \uparrow / AUC \downarrow / Accuracy \uparrow			
	ccMNIST	FairFace	YFCC100M-FDG	NYSEF
$\lambda_2 = 0.05$	0.53 / 0.75 / 98.61	0.57 / 0.63 / 95.99	0.88 / 0.55 / 88.31	0.86 / 0.57 / 61.71
$\lambda_2 = 1$	0.71 / 0.66 / 96.76	0.70 / 0.58 / 93.42	0.92 / 0.53 / 83.12	0.97 / 0.51 / 59.95
$\lambda_2 = 50$	0.72 / 0.63 / 89.07	0.78 / 0.52 / 88.65	0.95 / 0.51 / 72.63	0.98 / 0.51 / 55.28
$\gamma_1 = 0.025, \gamma_2 = 0.25$	0.47 / 0.79 / 97.07	0.53 / 0.60 / 93.99	0.88 / 0.55 / 88.69	0.86 / 0.56 / 61.71
$\gamma_1 = 0.25, \gamma_2 = 0.025$	0.66 / 0.75 / 88.54	0.62 / 0.58 / 93.06	0.91 / 0.54 / 81.49	0.86 / 0.57 / 58.03
$\gamma_1 = 0.025, \gamma_2 = 0.025$	0.71 / 0.66 / 96.97	0.70 / 0.58 / 93.42	0.92 / 0.53 / 83.12	0.97 / 0.51 / 59.95